PHILIPS

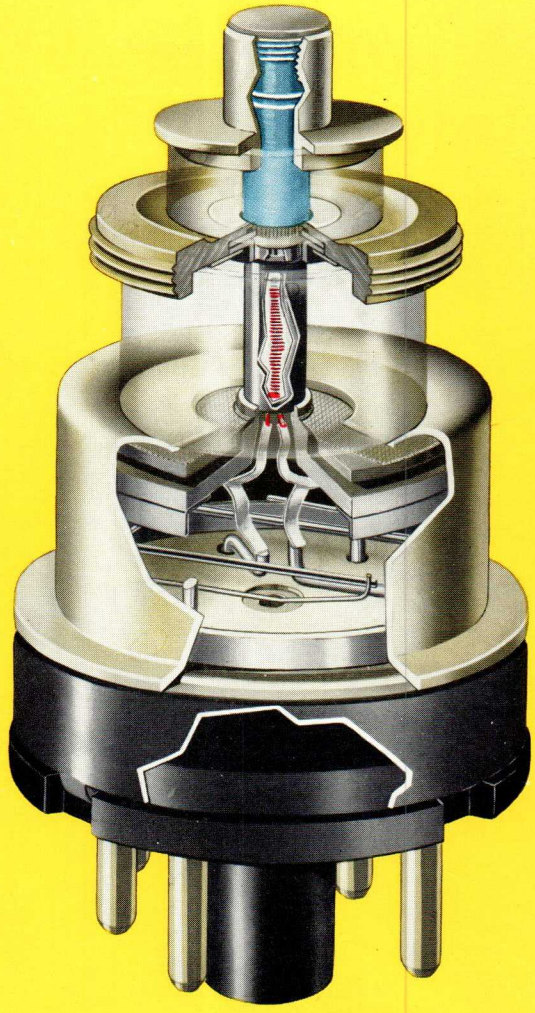

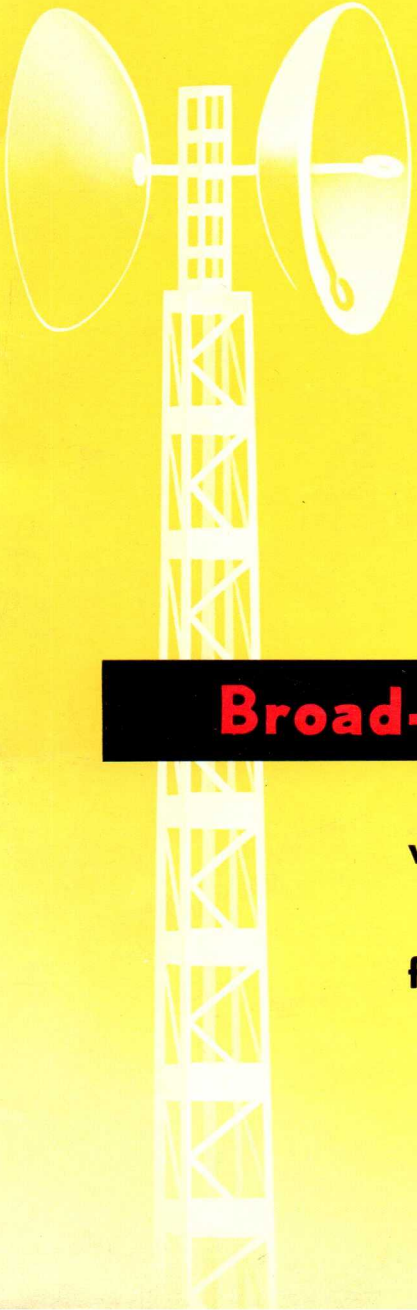

Broad-band 4000 Mc\s amplifier unit

with the triode **EC 56**
or **EC 57**
for microwave communication links

PHILIPS ELECTRONIC MARKETS DEPARTMENT

PREFACE

Point-to-point connections for transferring intelligence (e.g. audio, video, facsimile), such as AM, FM or pulse-coded modulation, may in principle consist either of wireless connections (beam transmitters) or of line connections (cables). The choice between these two systems will as a rule be determined by the local conditions in each individual case.

For wide-band transmission the use of a beam transmitter may be preferred to a line connection, because (expensive) coaxial cables and line-amplifiers can be dispensed with. Especially in cases where cables would have to be very long, or where their laying and maintenance would be difficult (rocky or watery areas), the beam transmitter is to be preferred to a line connection.

These arguments are valid both for multi-channel telephony and for TV link connections. Particularly in this application, which has become very up to date, the beam transmitter renders excellent and indispensable service. For semi-permanent link connections (commentaries) the beam transmitter is even the only practical solution.

For rapidly exchanging data, the beam transmitter will indubitably be appealed to, included the exchange between data-processing machines, the use of which may be expected to increase steadily.

Several types of electron tubes can be used as microwave amplifying tubes in beam transmitters. Proceeding development in the field of the short-wave technique has succeeded in manufacturing triodes, with their inherent advantages, for use on centimetric waves.

In this Bulletin a description is given of a 4000 Mc/s beam transmitter amplifier that can be equipped with the disc seal triodes EC 56 or EC 57. Due to the incorporation of a "ferrite isolator", a recent application of ferrites in microwave technique, it has been found possible to build the amplifier as a complete unit, the tuning and maintenance of which is extremely simple. As a consequence, an unlimited number of amplifiers can be connected in cascade, the EC 56 being used in the low-power stages and the EC 57 in the output stage.

Detailed information on these and additional merits of the amplifier is given in this Bulletin, whilst also the amplifier (type 88935) and the available accessoires, viz. the interstage isolator (type 88936/00 and the antenna isolator (type 88936/02), are described. In Appendices the theoretical considerations on which the design is based, are given in full detail.

CONTENTS

INTRODUCTION

The microwave amplifier with the EC 56/EC 57 described in this Bulletin is designed for use in beam-transmitter relay stations, which a.o.can provide the transmission of TV or telephony signals. Below, the specific properties of this amplifier are briefly discussed on the basis of the application mentioned above.

In beam transmitters use is made of the quasi-optical properties of very short radio waves, with the aid of which it is rather simple to produce narrow beams in which the transmitted power is highly concentrated. The C.C.I.R. [1]) has laid down directives for the application of relay stations, in which amongst others the frequency bands are allotted. One of these bands ranges from 3800 to 4200 Mc/s, for which band the amplifier in question has been designed. For the transmitter the F.M. system, the use of which has also been dictated by the C.C.I.R., has a great advantage over A.M., namely the high efficiency with which the microwave amplifiers can be operated.

Considering the choice of microwave amplifiers in relay stations, the following items will be of paramount importance.

BANDWIDTH, OUTPUT POWER, DISTORTION

In general the amount of information to be relayed is proportional to the bandwidth. With a view to a reasonable quality of a frequency-modulated TV signal, the bandwidth should amount to some tens of Mc/s. In multi-channel telephony the bandwidth is important in connection with the number of channels for which the band allows. The amplifier described has a bandwidth of 50 Mc/s between the 0.1 dB points, which is sufficiently large for the transmission of one TV channel or some hundreds of telephony channels.

The power transmitted in a given solid angle is determined by the output power of the transmitter and the antenna gain. For a good quality of reproduction this transmitted power should have a given minimum value, which is highly dependent on local circumstances, such as atmospheric absorptions and the distance to be bridged. Since this distance (scatter-propagation disregarded) is limited by the optical horizon, it will in practice amount to some tens of kilometres.

Another factor determining the minimum transmitted power is the noise factor of the receiver. The smaller this noise factor, the smaller the signal at the input of the receiver need be in order to obtain a given minimum signal-to-noise ratio at the output of the receiver.

---

[1]) Comité Consultatif International des Radiocommunications.

In practice it appears that an output of some hundreds of milliwatts is as a rule sufficient. The amplifier described, equipped with an EC 57, will deliver, at a power gain of 8 dB and a 0.1 dB bandwidth of 50 Mc/s, an output power of 1.8 W.

Although amplitude linearity of a frequency-modulated signal in itself is of no importance, a curved frequency-response characteristic gives rise to phase distortion ("level-to-phase conversion"). In order to reduce this type of distortion as much as possible, the amplifier described is so designed that the frequency response curve shows a horizontal part that, measured between the 0.1 dB points, has a width of 50 Mc/s (see Fig.1). An additional advantage of the flattened response curve is the possibility of connecting a number of amplifiers in cascade without any loss of bandwidth whatever.

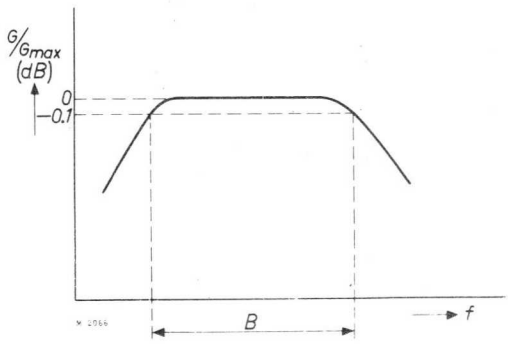

Another origin of phase distortion is found in group delay times. Their influence in the EC 56/EC 57 amplifier is, although it can completely be compensated, negligibly small [1]).

Fig.1. Frequency response curve of the amplifier described.

OPERATING VOLTAGE

The operating voltage of a relay station is of great importance in places devoided of a mains connection, such as sparcely populated areas or places that are difficult to approach (mountain tops etc.). The EC 56/EC 57 has an anode voltage of 180 V, which is in good agreement with those communication systems having a battery voltage of 200 V.

Furthermore a low operating voltage is of great interest for safety reasons, and with a view to insulation.

THE CONTINUITY OF THE TRANSMITTER

In view of the importance of link systems it is obvious that failures in relay stations have to be reduced to a minimum. In this respect the EC 56/EC 57 amplifier has the advantage that every amplifying stage of a cascade circuit is produced as a separate unit, so that it can be replaced at once. Moreover, all units of the cascade circuit are identically tuned and adjusted, so that they are mutually interchangeable. Adjusting the unit can therefore be brought about outside the transmitter, in which case a swept-frequency oscillator is an indispensable expedient (see page 19).

When during operation an amplifying tube breaks down, it can be replaced immediately, during which time the apparatus need not be switched off. Except for the tuning of the anode circuit no readjustments need be carried out before the transmission has come to an end.

---

[1]) See Appendix II.

DESCRIPTION OF THE AMPLIFIER

Basically the amplifier is a triode in grounded-grid circuit with tuned input and output circuits. These circuits (between grid and cathode and between grid and anode) are formed by quantities with distributed constants, whilst the input and output couplings are provided by waveguides. The basic set-up of the amplifier is shown in Fig.2.

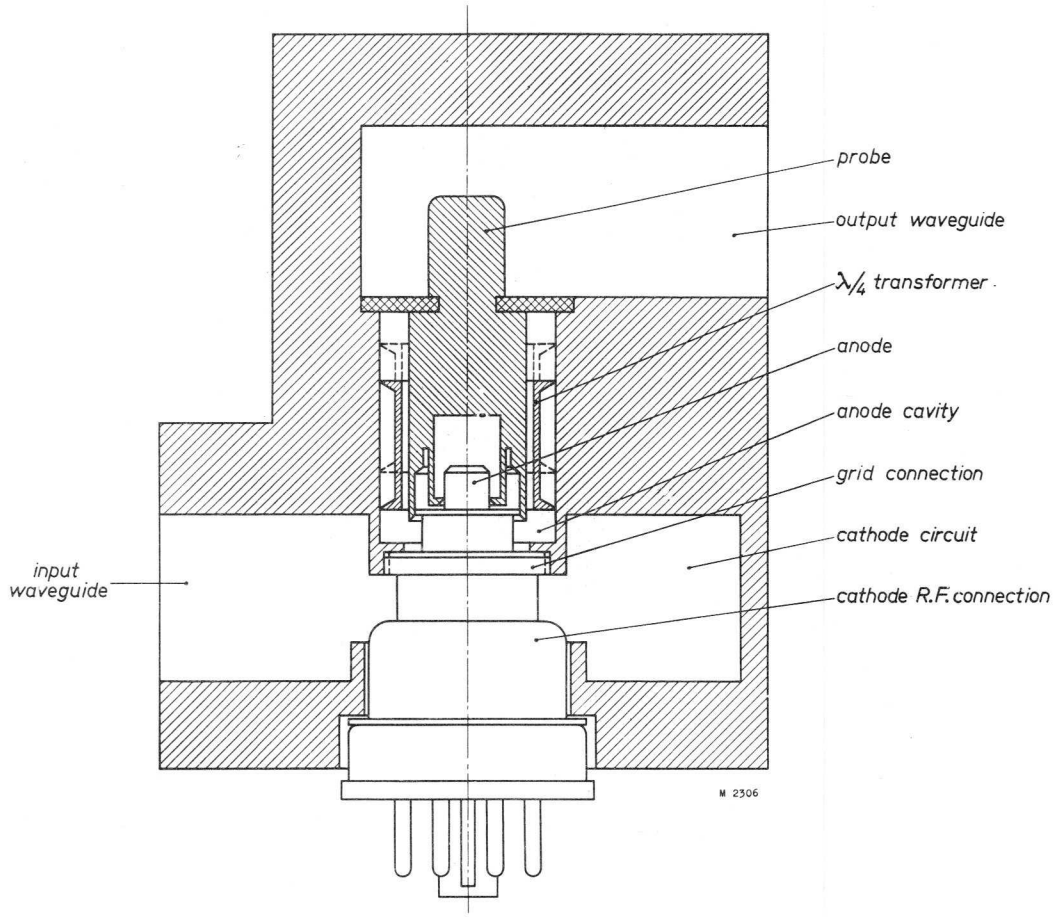

Fig.2. Simplified cross-section of the amplifier.

The cathode circuit is chiefly formed by a section of the input waveguide; the anode circuit consists of a cylindrical resonant cavity. This cavity is part of a bandpass filter (not indicated in Fig.2), which will be discussed in the following section.

The grid connection of the tube is screwed into the partition formed by the common wall of the cathode and anode circuits. This construction ensures a good R.F. contact between the grid connection of the tube and the circuitry, as well as a good separation between the two resonant circuits.

The anode cavity is tunable by means of a movable piston that, moreover, serves as a $\lambda/4$ transformer in the coaxial line which connects the cavity to the output waveguide. This transformer proved to be necessary to reduce the damping of the output waveguide on the cavity. The coupling between the coaxial line and the output waveguide is achieved by means of a probe functioning as a coaxial-to-waveguide transition.

As a result of the requirements made on the bandwidth and the power matching, the actual amplifier is more complicated than described above. Both the cathode and the anode side are provided with adjustable elements, whilst a ferrite isolator is connected to the output circuit to prevent reaction from the next stage having any unfavourable effect on the performance.

In the following Section the discussion of these elements will be based on their design.

THE CATHODE CIRCUIT

When considering the matching of the input side of the amplifier to the driver, the input impedance of the amplifier should be discussed first. The nature of this impedance is rather complicated; it can, however, with good approximation be represented by the equivalent circuit shown in Fig.3a. In this figure C_{KG} represents the cathode-to-grid capacitance, $1/S$ the electronic input damping of the tube (S = mutual conductance), L_K the inductance of the cathode and C_L the capacitance between the RF connections of grid and cathode.

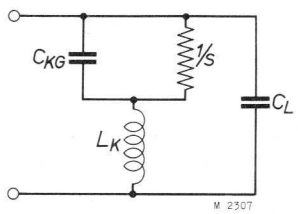

Fig.3a. Equivalent circuit of the input impedance.

It appears that at a given frequency within the band considered (approx. 3900 Mc/s) the total input impedance is real and equals the characteristic impedance of the input waveguide. This can be seen in Fig.3b, in which the impedances (admittances) of the components and their combinations are plotted in a Smith-diagram, normalized on the characteristic impedance of the input waveguide.

It is obvious that such a correct matching as indicated in Fig.3b exists at one frequency only. The deviations occurring at other frequencies are shown in Fig.4, in which curve *I* represents the input admittance of the amplifier with the frequency as parameter and the anode short-circuited for R.F.

Fig.4 shows that between 3800 Mc/s and 4000 Mc/s the mismatching is relatively small, whereas above 4000 Mc/s the V.S.W.R. in the input waveguide assumes rather high values. In the amplifier the mismatching is corrected by means of a variable impedance transformer inserted in the input waveguide. To avoid a too heavy reduction of the bandwidth the transformer ratio must not be excessive. At frequencies above 4000 Mc/s the input waveguide is therefore provided with a fixed reactance, which results in reducing the mismatching in such a way that the values of the frequency in Fig.4,

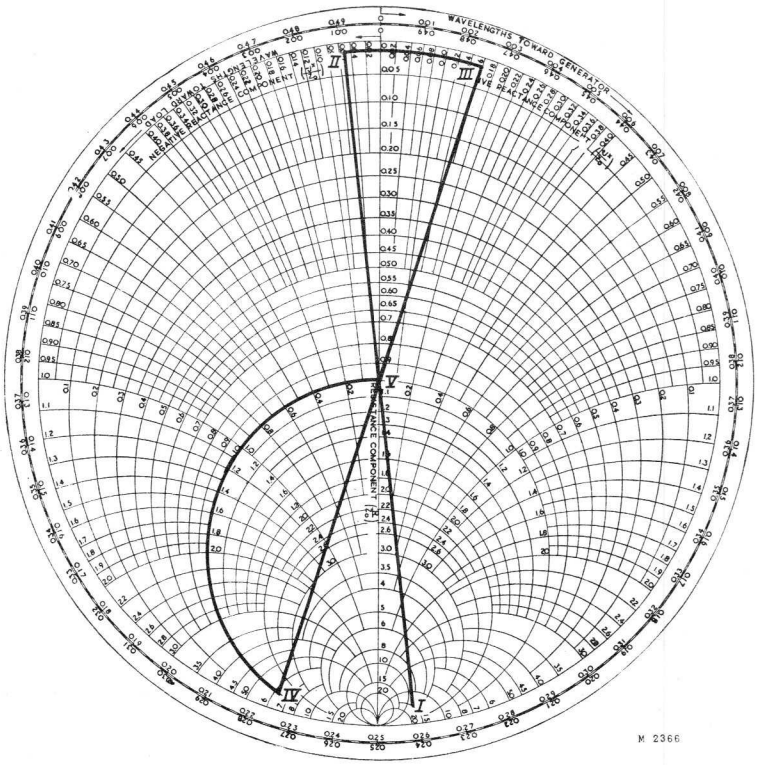

Fig.3b. Impedances and admittances of the elements of Fig.3a, plotted in a Smith-diagram, and normalised on the waveguide admittance. The reference plane passes through the axis of the tube. *I*: $S + j\omega C_{KG}$; *II*: $1/(S + j\omega C_{KG})$; *III*: *II* + $j\omega L_K$; *IV*: $1/(II + j\omega L_K)$; *V*: *IV* + $j\omega C_L$.

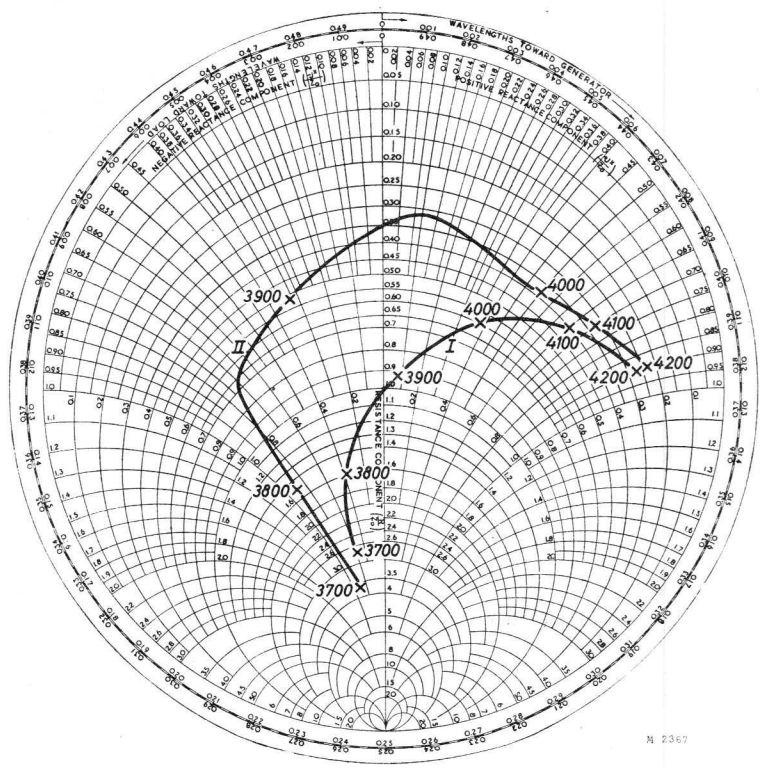

Fig.4. Input admittance of the amplifier plotted in a Smith-diagram with the frequency as parameter; *I*: anode circuit short circuited, *II*: anode circuit tuned to the operating frequency.

curve *I*, are increased by 200 Mc/s. Due to the presence of the additional reactance, the part of curve *I* located between 3800 and 4000 Mc/s is now valid for the frequency range from 4000 to 4200 Mc/s. The remaining mismatch can be corrected with the aid of the variable impedance transformer.

The fixed reactance discussed consists of two matching strips inserted in the input waveguide close to the cathode RF connection of the tube.

In the preceding the input impedance has been considered with the anode short-circuited. When, however, the anode circuit is tuned to the operating frequency, which is actually done, a reaction occurs, as a result of which the input admittance deviates from curve *I* of Fig.4. This can be seen in curve *II*, showing the input admittance with tuned anode circuit [1]).

The total reaction is the combination of three effects, viz.: (1) reaction via the electron current in the tube, (2) capacitive reaction via the anode-to-cathode capacitance, and (3) inductive coupling between the anode and cathode circuits via the grid wires of the tube.

The deviation of curve *II* with respect to curve *I* depends strongly on the value of the amplification factor (μ) of the tube: the higher the value of μ, the smaller the deviation will be. Tubes with a high μ would therefore be preferable as far as small mismatching and consequently small reduction of the bandwidth are concerned. Output and gain are, however, unfavourably affected by a high amplification factor. The EC 56/EC 57 has therefore been so designed that the value of its amplification factor gives a reasonable compromise between bandwidth on the one hand, and power gain and output power on the other.

As a result of the heavy damping by the small input impedance of the tube, the bandwidth of the cathode circuit is relatively large. The overall bandwidth of the amplifier is therefore mainly determined by the bandwidth of the anode circuit.

THE ANODE CIRCUIT

As was mentioned in the preceding, a bandpass filter is incorporated in the anode circuit of the tube. The filter consists of two resonant circuits and a coupling element. One of these circuits is the anode cavity; the other is formed by a resonant iris inserted in the output waveguide, whilst the coupling element consists of the waveguide section that is located between the resonant circuits and is provided with a variable reactive element.

From measurements it follows that, at tuned anode circuit and disconnected coupling element and iris, the output damping of the amplifier is very small. This is to be attributed to the positive feedback occurring when the anode cavity is tuned. The apparent quality factor of the latter may therefore be regarded as being very high.

---

[1]) In this respect "anode circuit" means the bandpass filter with a flattened response curve, the 0.1 dB bandwidth of which is 50 Mc/s (see next Section: "The anode circuit").

From calculations on the bandpass filter (see p.42) a condition has been derived that must be satisfied in order to have a response curve with maximum flatness [1]). Furthermore, it appears that with such a response curve the 0.1 dB bandwidth of the bandpass filter is *exclusively* determined by and directly proportional to the 3 dB bandwidth of the second resonant circuit (iris), provided the quality factor of the first resonant circuit (cavity) is infinitely high. Although the actual quality factor of the anode cavity has a finite value, in practice the statement mentioned above also holds for the case in question. Thus the amplifier has the important feature that its 0.1 dB bandwidth is practically independent of spreads in tube data, whilst its bandwidth can be adjusted by the choice of a given iris.

The iris, which forms an integral part of the amplifier assembly, consists of two cylindrical matching strips and a tuning screw located in the output waveguide. With the aid of the tuning screw the iris can be tuned to the desired frequency.

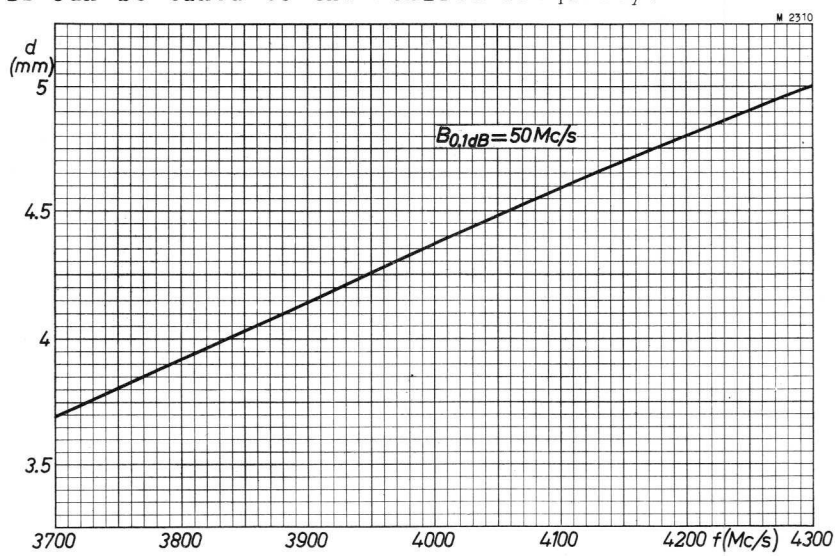

Fig.5. Relationship between the diameter of the matching strips of the resonant iris and the resonant frequency for a 0.1 dB bandwidth of the amplifier of 50 Mc/s. The value for the diameter is also valid for the average diameter of two unequal strips.

At a constant configuration of the iris its bandwidth depends on the resonant frequency. Since the bandwidth is determined by the diameter of the (inductive) matching strips, the latter have been made interchangeable, so that for every frequency within the band the 0.1 dB bandwidth of the amplifier can be adjusted to 50 Mc/s. This relationship between strip diameter and resonant frequency is shown in Fig. 5.

THE FERRITE ISOLATOR

It is well known that at microwaves non-reciprocal phenomena can be realised with the aid of ferrites. Advantage is taken of this property in the so-called "ferrite isolator", a fourpole causing in one direction a low, and in the opposed direction a high attenuation. The performance of this isolator is based on the occurence of gyro-magnetic resonances in ferrites [2]).

[1]) See Appendix I, Section 3.

[2]) *H.G.Beljers*, Amplitude Modulation of Centimeter Waves by means of Ferroxcube, Philips Techn.Rev., Vol.18, p.82 (No.3).

In the EC 56/EC 57 amplifier the ferrite isolator is used for preventing undesired feedback (reflections), caused by incorrect matching of the following stage (amplifier or antenna).

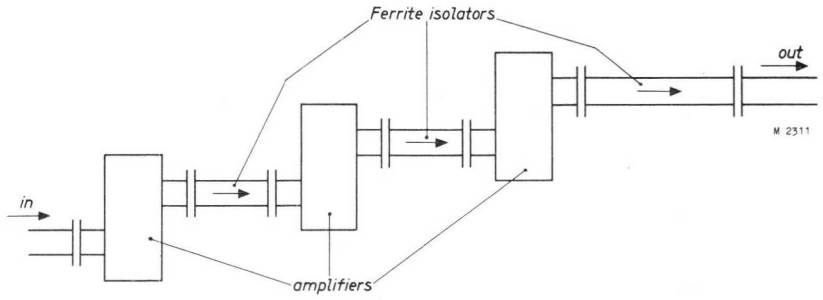

Fig.6. Schematic representation of the cascade circuit of three amplifiers with ferrite isolators.

The set-up of a multi-stage amplifier with the application of ferrite isolators is schematically shown in Fig.6. The isolators are so connected that power propagated in the direction of the arrow is passed practically unattenuated. In the opposite direction a large attenuation occurs (20 to 40 dB). Reflections, caused by a following stage, are therefore heavily attenuated and have no influence whatever on the behaviour of the preceding amplifier. The unit amplifier-isolator can therefore be considered as being unidirectional. As a result, each of these units can be adjusted separately, which renders the complete adjustment of the multi-stage amplifier very simple.

The ferrite isolator (see Fig.7) consists of a waveguide section, in which a slab of ferroxcube is mounted in the direction of propagation. This slab is magnetized by a permanent magnet outside the waveguide. Since the field strength needed for the occurrence of gyro-magnetic resonance depends on the frequency of the microwave signal, the former has been made adjustable with the aid of a variable reluctance.

In order to increase the ratio between the attenuations of the incident and the reflected wave, a plate of quartz is cemented to the ferroxcube slab. For matching purposes either side of the isolator is provided with two tuning screws.

In order to check the amount of power passing the ferrite isolator, one of the side walls is provided with an aperture through which a small coupling loop can be inserted in the isolator. It is preferable to solder this loop onto a coaxial connector, type number UG 53 U, which can be mounted directly on the isolator. When the aperture is not used, it must be closed by a cover plate.

THE ANTENNA ISOLATOR

The ferrite isolator connected between the final amplifier and the load (antenna) is provided with a tapered quartz plate as a result of which the reflection of this "antenna isolator" is smaller than that of an "interstage isolator". As a consequence, it is also made somewhat longer (Fig.8).

Since the configuration of the antenna isolator is somewhat different from that of the interstage isolator, two additional matching strips are inserted at both sides.

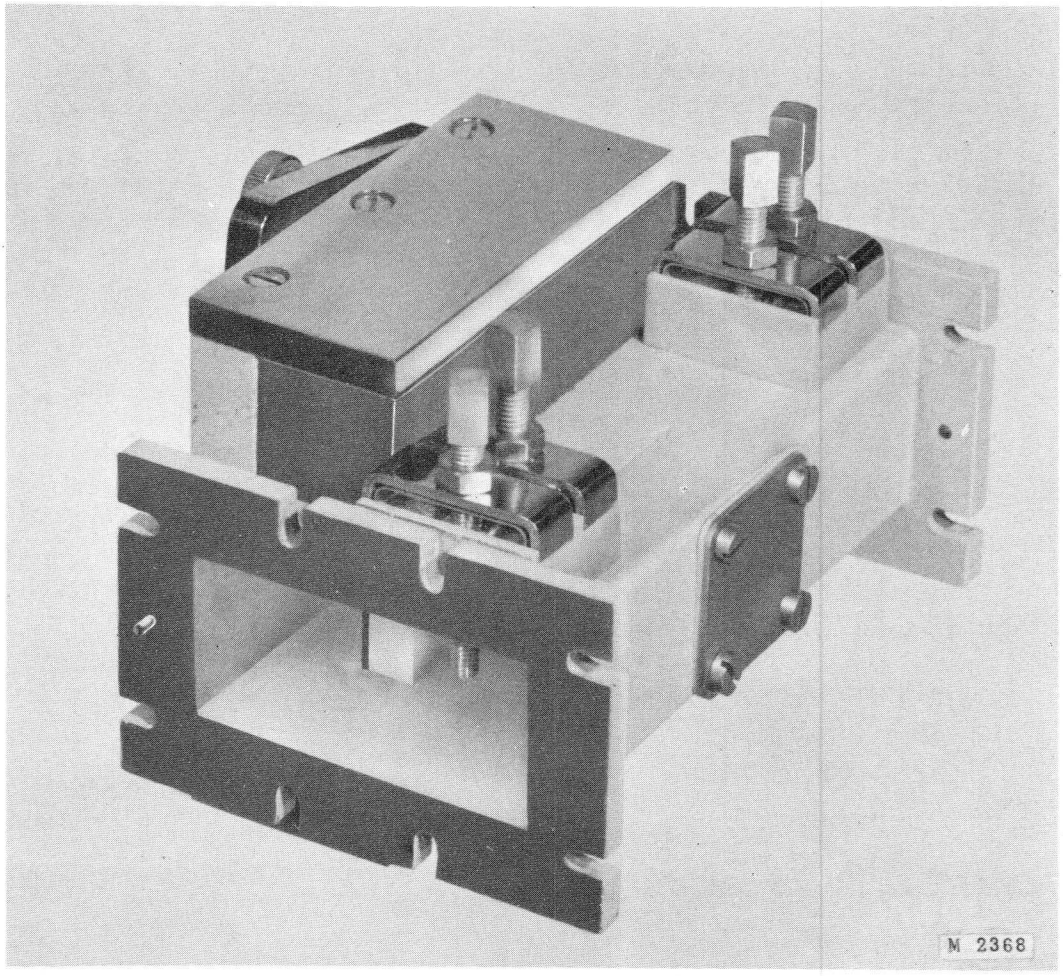

Fig.7. Photograph of the interstage isolator.

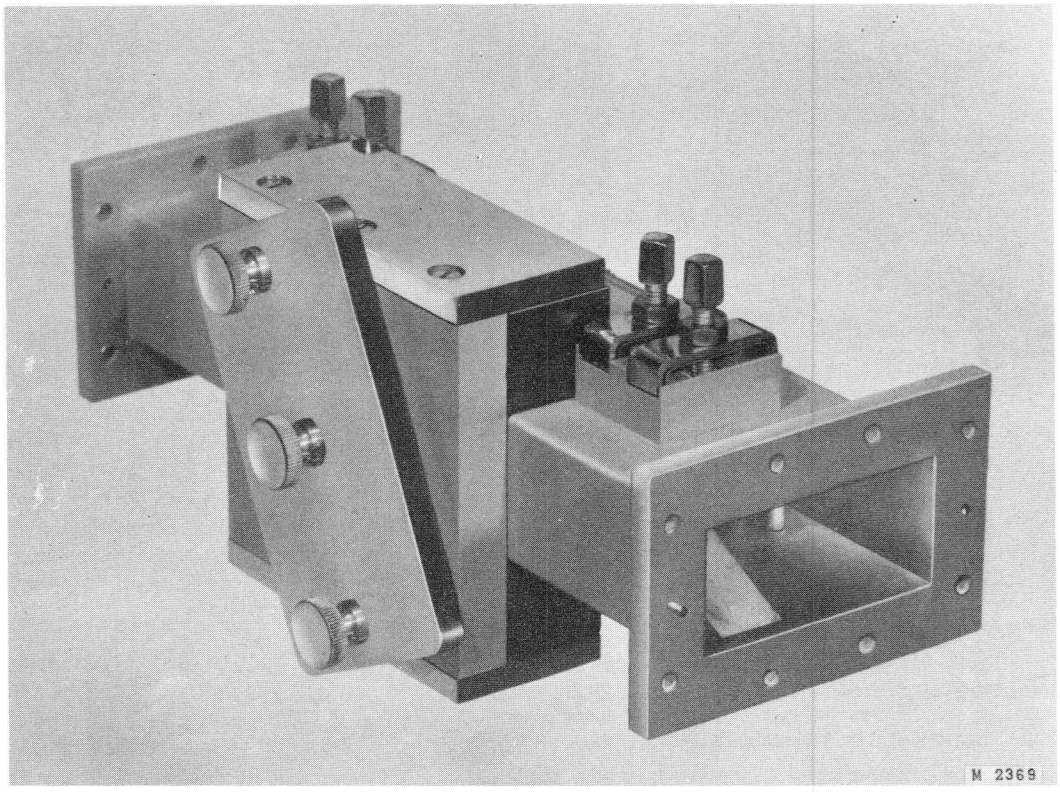

Fig.8. Photograph of the antenna isolator.

CONSTRUCTIONAL DETAILS

The main part of the amplifier consists of a brass block provided with several apertures and cover plates at the top and at the bottom.

The input and output waveguide, which are formed by apertures in the block, run parallel and end at opposite sides of the block (see Fig.9). Standard 7.5 cm waveguides (RETMA WR187, JANMIL RG-49U, RG-95U, RCL 351 type WG12) can be connected to the block by means of standard screws (M3). In Fig.9 the opening of the output waveguide points to the front.

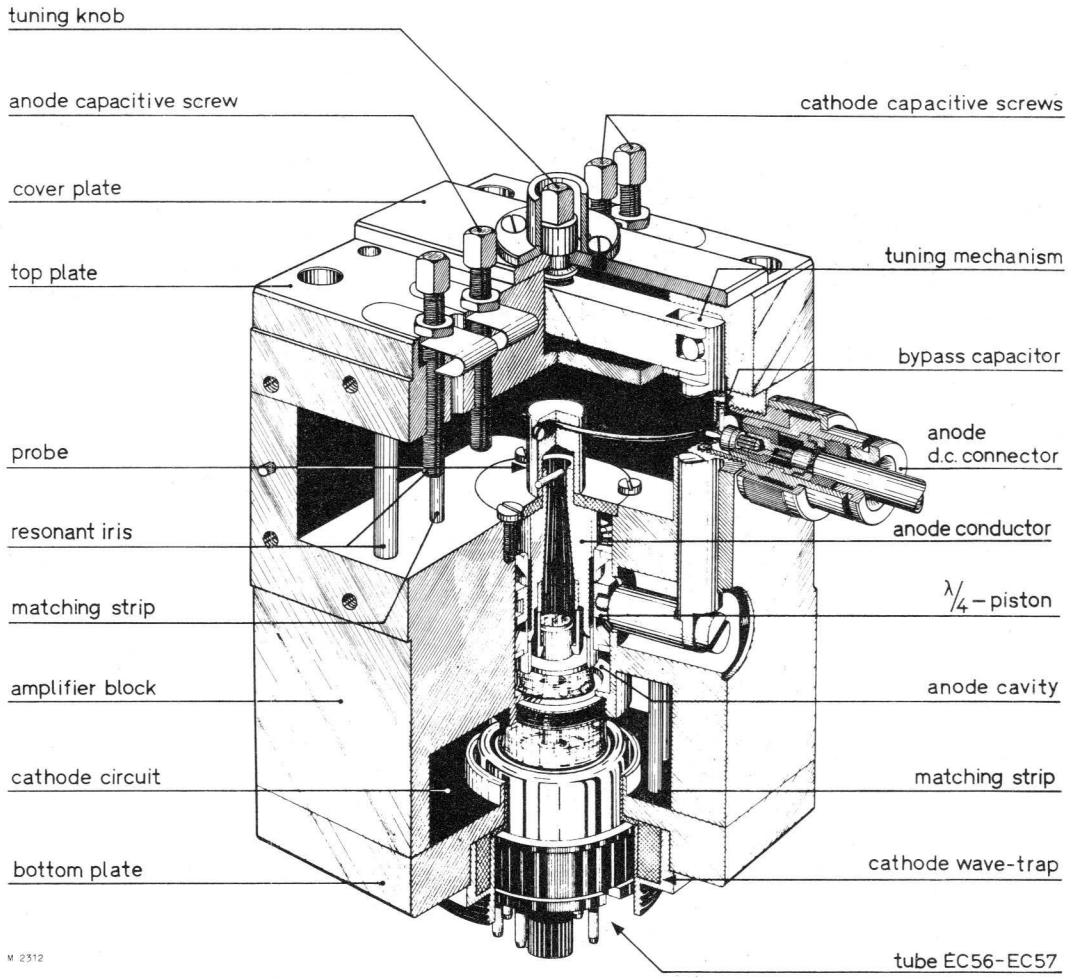

Fig.9. Cut-away view of the amplifier block.

By screwing the tube into the block, the grid and the cathode RF connections are connected to the upper and lower faces respectively of the input waveguide. The grid has a galvanic connection with the block, whereas the coupling of the cathode RF connection is established via a wave trap in such a way that these electrodes are mutually isolated for d.c.

The cathode circuit of the amplifier is formed by the short-circuited part of the input waveguide; in Fig. 9 this part is seen at the front. The distance between the short circuit and the axis of the tube is approx. $\lambda_g/4$ at 4000 Mc/s. Fig.9 also shows the matching strips that reduce the mismatching between 4000 and 4200 Mc/s.

The impedance transformer, which consists of two matching strips and two tuning screws, is situated between the cathode connection and the input of the amplifier. These screws can be operated from the top of the amplifier assembly.

When the tube is inserted in the block, the anode connection of the tube is enclosed by a resilient ring, which forms part of the inner conductor of the coaxial line. The outer conductor of the latter is formed by a piston. Since part of the wall of the anode cavity is formed by the piston, the volume and consequently the resonant frequency of the cavity is varied by shifting the piston. Tuning is achieved by turning a screw at the upper side of the amplifier block, the screw being connected to the piston via a cross bar and two connecting rods.

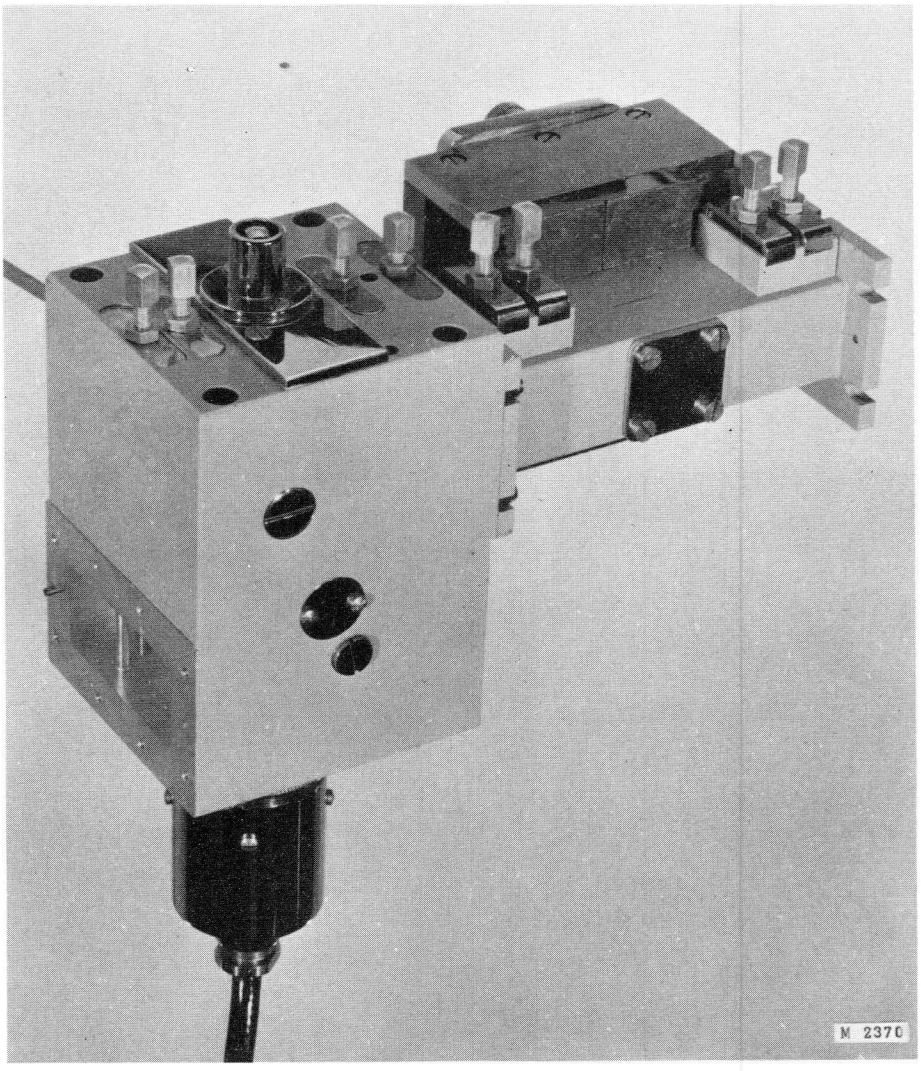

Fig. 10. Photograph of the complete amplifier unit, consisting of amplifier block and ferrite isolator.

The cylindrical inner conductor ends in a probe, which establishes the coupling with the output waveguide. The anode supply voltage is fed to the probe via a thin wire and a plug, which, moreover, functions as a feed-through capacitor.

The variable susceptance in the output waveguide between the probe and the iris consists of a matching strip combined with a tuning screw. The latter is operated from the top of the amplifier block, similar to the tuning screw of the iris.

The five variable elements can be operated with a square 5 mm socket wrench. To avoid backlash, leaf springs and nuts are provided.

The air inlet is formed by a hose pillar, protruding from one side wall of the block. The air flows through the anode cavity and the

hollow inner conductor of the coaxial line transformer into the output waveguide. The duct between the inlet and the cavity forms a cut-off waveguide, so that no power is lost.

Both the d.c. anode connection and the cooling air inlet can be mounted at either side of the block. The apertures not in use are sealed by screws.

The heater voltage and the direct cathode voltage are fed to the tube via a cable and socket, secured to the bottom of the block by a cap nut.

Fig.10 shows the amplifier block with the interstage ferrite isolator connected to it.

MECHANICAL

Finish

The outer surfaces of the amplifier and ferrite isolator are either nickel-plated or lacquered. The inner parts carrying RF currents are silver-plated, with the exception of the anode cavity, the walls of which are gold-plated.

Dimensions

The overall dimensions of the amplifier block are:

Length (without ferrite isolator)	74	mm
Width (air inlet included)	96	mm
Height (bottom plug included; controls in upper position)	210	mm
Length of the interstage isolator	102	mm
Length of the antenna isolator	170	mm

Weights

Amplifier block with tube	3.40	kg
Interstage isolator	1.35	kg
Antenna isolator	1.55	kg

ELECTRICAL DETAILS

POWER GAIN AND OUTPUT POWER

In Fig.11 the output powers of the EC 56 and the EC 57 are plotted as functions of the driving power. These values have been measured in the amplifier described. Lines of constant power gain are also indicated in the figure.

As appears from Fig.11, the power gain of the tubes is constant at low level. The bend of the characteristic of the EC 56 begins earlier than that of the EC 57, so that the latter tube is more suitable for higher output powers than the EC 56. The EC 56, however, can be used advantageously at low level and as a driver preceding an amplifier equipped with the EC 57.

The characteristics of Fig. 11 are valid for one frequency only (3900 Mc/s). In the entire frequency band from 3800 to 4200 Mc/s the low-level power gain varies according to Fig.12. In this figure the discontinuity occurring at 4000 Mc/s is due to the additional matching strips with which the input waveguide of the amplifier is provided in the range above 4000 Mc/s. As in Fig.11, the 0.1 dB bandwidth in Fig.12 is 50 Mc/s.

ATTENUATION AND BANDWIDTH OF THE FERRITE ISOLATORS

The values in Fig.11 and Fig.12 are valid only for the amplifier itself. When ferrite isolators are used , their forward attenuation should therefore be taken into account. The electrical data of both the interstage and the antenna isolator are tabulated below.

	interstage isolator	antenna isolator
Forward direction attenuation	max. 1 dB	max. 1 dB
Backward direction attenuation at centre frequency (as adjusted with the magnetic series impedance)	min. 30 dB	min. 30 dB
Bandwidth between the 20 dB attenuation points	min. 250 Mc/s	min. 250 Mc/s
Voltage standing wave ratio at centre frequency	1	1
Voltage standing wave ratio within 100 Mc/s above and below centre frequency	max. 1.1	max. 1.03

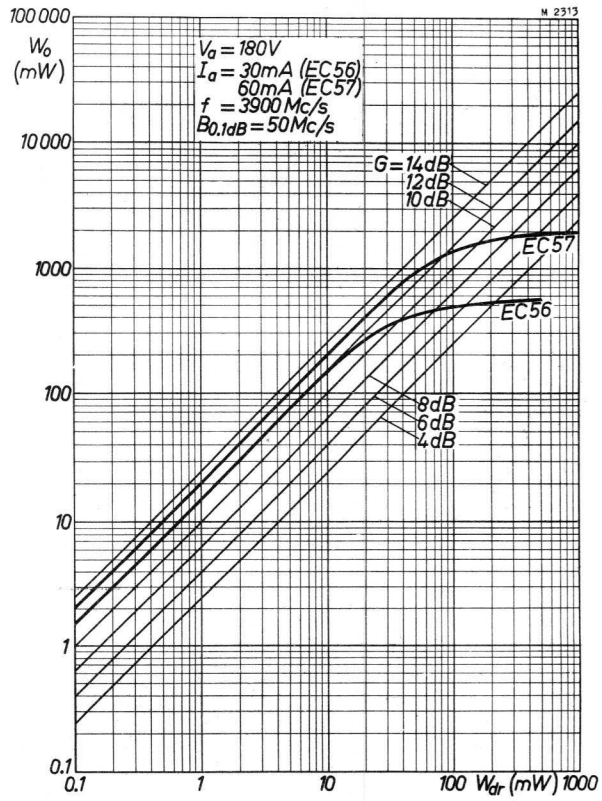

Fig.11. Output power of the EC 56 and EC 57 as a function of the driving power with lines of constant power gain.

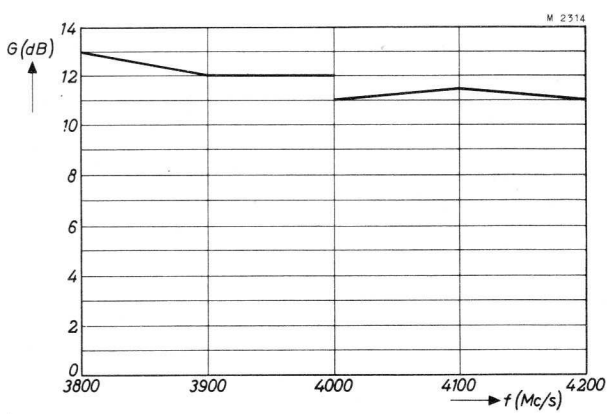

Fig.12. Low-level power gain of the EC 56 as a function of the frequency.

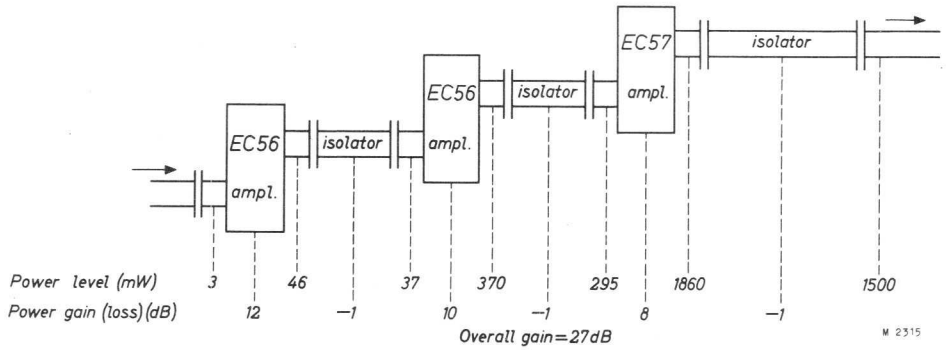

Fig.13. Power level and power gain (loss) in a 3-stage amplifier equipped with two tubes EC 56 and one tube EC 57 and provided with two interstage isolators and one antenna isolator.

As an example of the performance of some amplifiers circuited in cascade, a 3-stage amplifier is schematically indicated in Fig.13 with data of the power levels and power gains (losses) as they are derived from Fig.11. For the attenuation of the ferrite isolators the maximum value of 1 dB has been assumed.

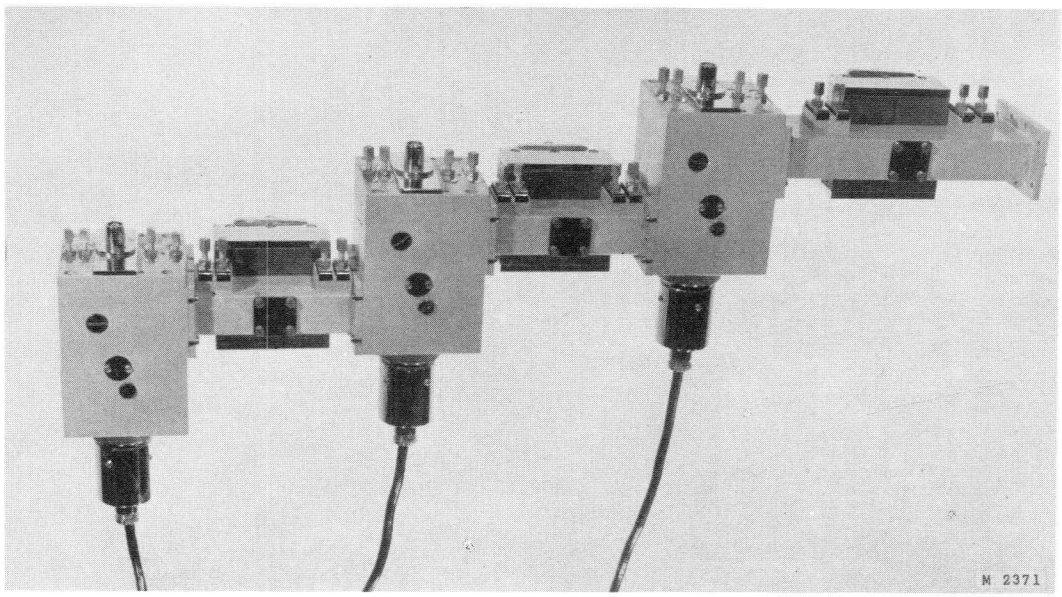

Photograph of the three-stage amplifier with ferrite isolators according to the schematical representation in Fig.13.

ADJUSTMENT OF THE AMPLIFIER AND THE FERRITE ISOLATORS

THE MEASURING AND TEST SET-UP

As was mentioned before, one of the features of the EC 56 amplifier is the possibility of adjusting each unit independent of the remainder of the apparatus. This adjustment can be carried out very simply and quickly in the set-up, a photograph and a block diagram of which are shown in Figs 14 and 15 respectively. In this set-up the ferrite isolators can also be adjusted.

The method of adjustment is based on the use of a swept-frequency oscillator (wobbulator), which can be seen at the left of Fig.14 and delivers a frequency-modulated signal to the waveguide test bench, in which the device under test is inserted. The centre frequency of the oscillator can be varied from 3700 to 4300 Mc/s, whilst a constant output power of approx. 1 mW is available over a frequency sweep of maximum 500 Mc/s; the deviation from the value of 1 mW proved to be less than 0.3 dB within the frequency sweep specified.

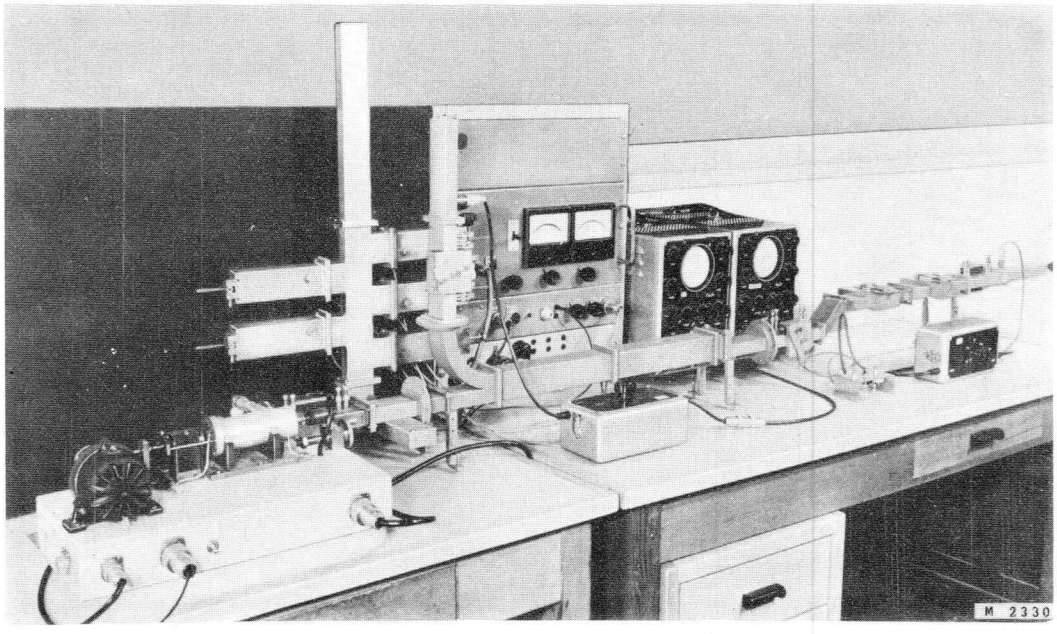

Fig.14. Measuring equipment for adjusting the units.

The signal from the swept-frequency oscillator is fed to the test bench via a coaxial line and a coaxial-to-waveguide transition. Between this transition and the device under test a ferrite isolator and two directional couplers are interposed. The ferrite isolator prevents frequency pulling of the oscillator due to mismatching of the object under test. The output power from the object is applied to a detector via two calibrated variable attenuators and a ferrite isolator. The detected signal is amplified and fed to the vertical plates of a cathode-ray oscilloscope (Osc_2). The horizontal deflection voltage of this oscilloscope is obtained from the swept-frequency oscillator, and is proportional to the frequency, so that the frequency response curve of the object under test is displayed.

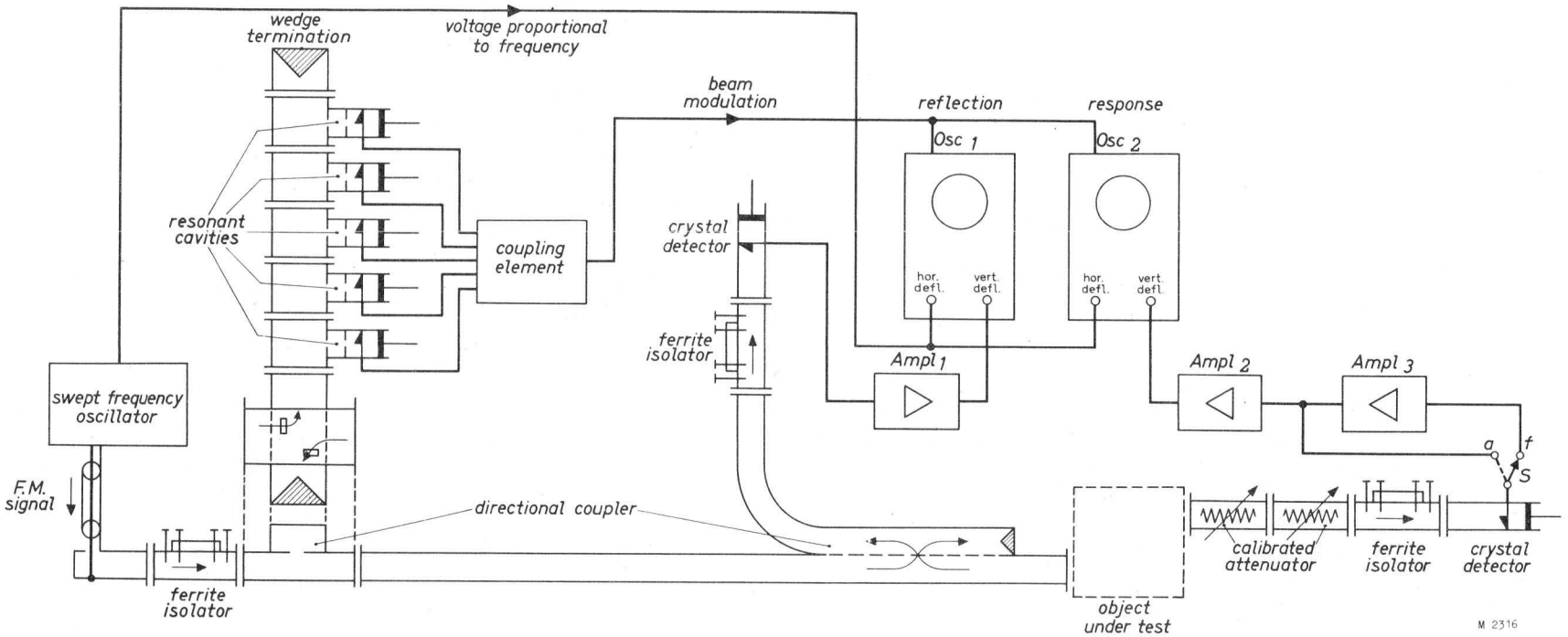

Fig.15. Block diagram of the measuring and test set-up.

One of the directional couplers, placed before the device, detects the reflected power. Similar to the output power of the device, the detected signal from the directional coupler is applied to a cathode ray oscilloscope (Osc_1), the horizontal deflection of which is identical to that of Osc_2. In this way the reflected power as a function of the frequency is displayed on the screen of Osc_1.

During the fly-back of the electron beam of the oscilloscopes the power output of the swept-frequency oscillator is suppressed so that lines of zero output and zero reflection are shown on the respective screens. In order to keep these lines at a constant height, d.c. restoration of the vertical deflection voltage is applied. For this reason both oscilloscopes, which can be of the normal A.F. type, are provided with an additional diode circuit.

In the oscilloscopes brightness modulation is also applied, resulting in marking spots on the screen, which indicate some discrete frequencies. These marking spots emanate from five resonant cavities coupled to the first directional coupler. Each cavity is provided with a crystal detector in which a voltage is induced as soon as the instantaneous frequency of the swept-frequency oscillator coincides with the resonant frequency of the cavity under consideration. Via a coupling network the detectors are connected to the beam modulation electrode of the oscilloscopes. During the modulation cycle the cavities, which are tuned to different frequencies, one after another come into resonance. As a result, local brightness variations occur on the screens of the oscilloscopes, corresponding to the frequencies to which the cavities are tuned.

With a view to the different dimensions of the amplifier and the ferrite isolators, it is preferable to use connectors to compensate for the different lengths and heights.

Before discussing the measuring procedure, a detailed description will be given of the swept-frequency oscillator mentioned above.

THE SWEPT-FREQUENCY OSCILLATOR

CIRCUIT DESIGN

It proved to be most convenient to equip the swept-frequency oscillator with a reflex klystron, because with this type of tube it is comparatively easy to obtain a constant output over a fairly broad frequency range. To ensure that the tube oscillates with a constant output it is, however, necessary for the repeller voltage to vary with the resonant frequency of the oscillator circuit.

This may be explained with reference to Fig.16 in which the repeller voltage of the klystron has been plotted as a function of the resonant frequency of the circuit, with lines of constant output as parameter. In the shaded areas the klystron does not oscillate. If a frequency sweep of $\pm\Delta f$ occurs at the centre frequency f_o, and the repeller voltage is V_o, the input will vary as a function of the frequency as indicated in the lower part of the diagram. It will be clear that this would result in the output power P_o depending to an inadmissible extent on the frequency f.

To obtain a constant output P_o within the frequency range from f_1 to f_2, the repeller voltage should vary from V_1 to V_2 so that the line PQ is followed. The line appears to be straight, so that a linear relation exists between the resonant frequency f and the required repeller voltage V_{rep}.

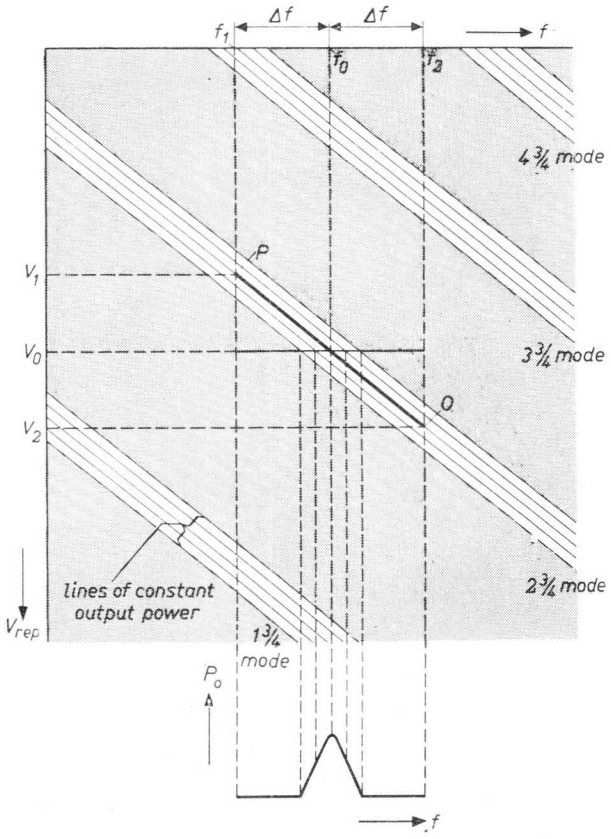

Fig.16. Diagram representing the repeller voltage of the reflex klystron as a function of the frequency with lines of constant output power as parameter. In the shaded areas no oscillations are produced.

It will be shown below how use is made of the fact that the output is zero in the shaded part of the diagram.

The resonant circuit of the oscillator consists of a coaxial pair, the resonant frequency of which can be modified by means of a piston. Fig. 17*a* gives a schematical representation of the resonant circuit, whilst the resonant frequency has been plotted as a function of the location of the piston in Fig.17*b*. Within the frequency sweep used, this dependency may be considered to be linear. (The fully drawn line in Fig. 17*b* actually forms part of a hyperbola since the location of the piston is linearly related to the resonant wavelength).

It has thus been shown that the resonant frequency is linearly related both to the required repeller voltage for a constant output and to the location of the piston. Consequently, the relation between the required repeller voltage and the location of the piston is also linear. It is therefore possible to derive the repeller voltage from the location of the piston by means of a rather simple electronic circuit.

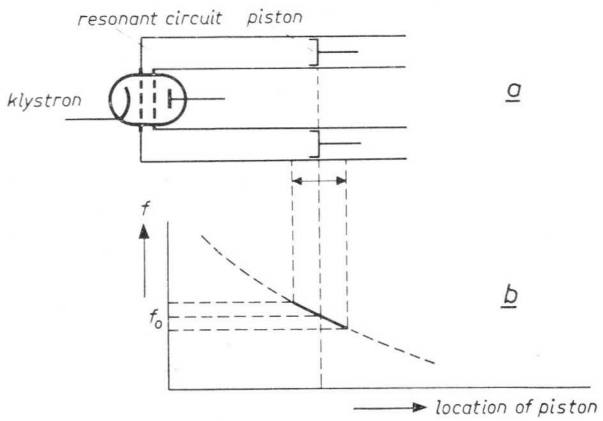

Fig.17. (*a*) Schematic representation of the resonant circuit of the klystron oscillator, (*b*) relation between the location of the piston and the resonant frequency.

OPERATION AND CONSTRUCTION

The operation of the circuit will be explained with reference to Fig.18 in which the block diagram is shown, and to Fig.19 which gives the relations between the various quantities.

The piston of the oscillator is linked by means of connecting rods to an eccentric mounted on the spindle of a small motor. If this spindle rotates at a uniform speed the piston will describe a substantially harmonic vibration as shown by Fig. 19*a*, in which the location of the piston has been plotted as a function of time (*T* denotes the duration of one rotation).

Fig.19*b* represents the relation between the location of the piston and the resonant frequency of the oscillator circuit. The resonant frequency as a function of time has been plotted in Fig.19c.

The oscillatory condition for a constant output represented by Fig.19*d* and the relation $f = f(t)$ given by Fig.19c determine the required variation of the repeller voltage as a function of time (Fig.19e, complete sinusoidal curve).

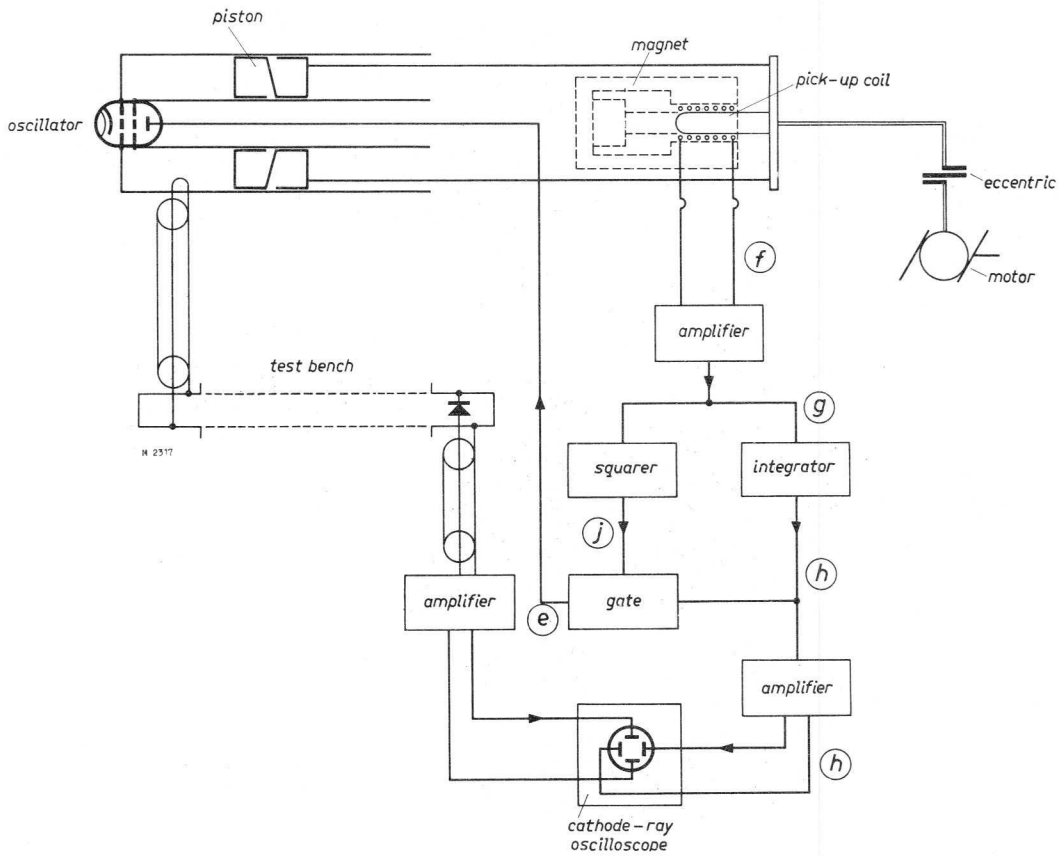

Fig.18. Block diagram of the complete test equipment.

Comparison of Figs19a and e shows that the repeller voltage varies linearly in phase with the location of the piston. In principle, it should therefore be possible to obtain a control voltage by ganging a linear potentiometer with the connecting rod of the piston, but this is impracticable for mechanical reasons. Therefore a small coil is used which is fixed to the piston rod and located in the field of a permanent magnet. A voltage is thus induced in this coil if it is moved to and fro; in Fig.19*f* the magnitude of this voltage has been plotted as a function of time. This voltage is the derivative of the enclosed flux (which is proportional to the location of the piston) with respect to time. To give the signal controlling the potential of the repeller the correct phase, this voltage must therefore be integrated. After the voltage induced in the coil has passed through an amplifier in which its phase is reversed, this integration is achieved by means of an *R-C* network. Fig.19*g* shows the signal at the output of the amplifier and Fig.19*h* the integrated signal.

To obtain the correct form for the repeller voltage, the phase of the signal according to Fig.19*h* should be reversed once again. This is achieved in the gate circuit which has been incorporated to obtain a reference line of zero output on the screen of the cathode-ray tube.

To the control electrode of the gating tube, which determines whether the input signal (Fig.19*h*) is passed or not, a square-wave signal according to Fig.19*j* is applied. This signal is positive during the interval from $T/4$ to $3T/4$ and negative during the other half cycle. The output voltage of the gate circuit, which is applied to the repeller of the klystron, will assume the form of the fully drawn curve of Fig.19e. (The phase of the signal shown in Fig.19*j* is reversed, similar to that of the signal shown in Fig.19*h*.)

The value of the repeller voltage is so adjusted that during the half cycle that the gate is closed, the relation between the repeller voltage and the resonant frequency of the oscillator circuit is such that the klystron will not oscillate. The fully drawn line in Fig.19*d* represents the cycle passed, with the time t as parameter.

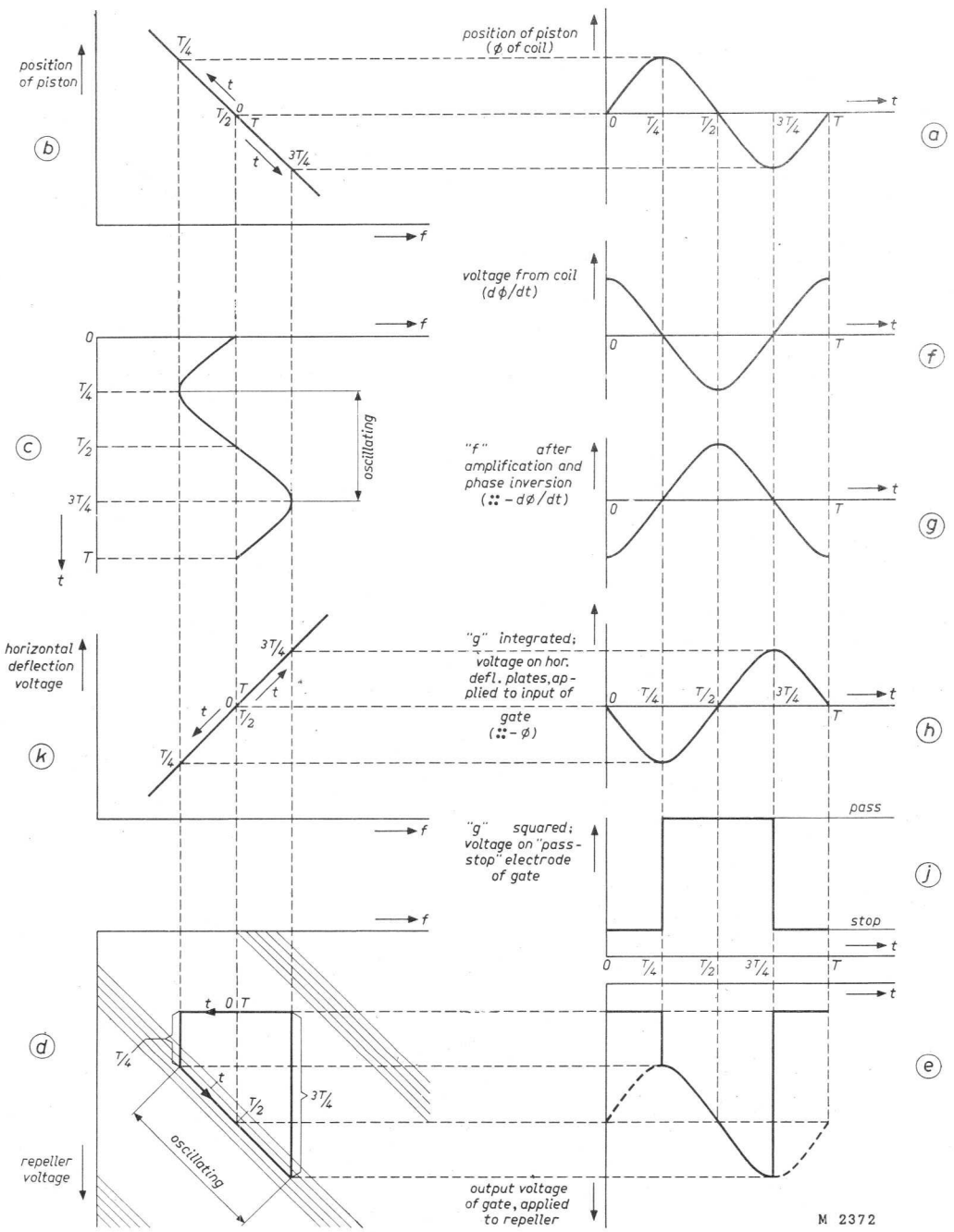

Fig.19. Relationships between the various quantities marked in accordance with the block diagram of Fig.18.

The square-wave signal required for controlling the gate circuit is supplied by a squarer to which a signal of the type shown in Fig.19*g* is fed.

The voltage for the horizontal deflection of the oscilloscope should be proportional to the frequency. This condition is satisfied by the integrated voltage of Fig.19*h*, as shown by Fig.19*k* representing the relation between the signals of Figs 19 c and *h* with the time as parameter. After having been amplified, the output voltage of the integrating network is applied to the horizontal deflection electrodes of the oscilloscope.

The rotational speed of the motor should be high enough for the brightness fluctuations of the image not to be annoying. On the other hand, this speed may not be too high, since the forces due to inertia could then become excessive. A speed of 1500 r.p.m. proved to give satisfactory results.

MECHANICAL CONSTRUCTION OF THE OSCILLATOR

Figs 20 and 21, which illustrate the assembled and the partly dismounted apparatus, clearly show the construction of the oscillator.

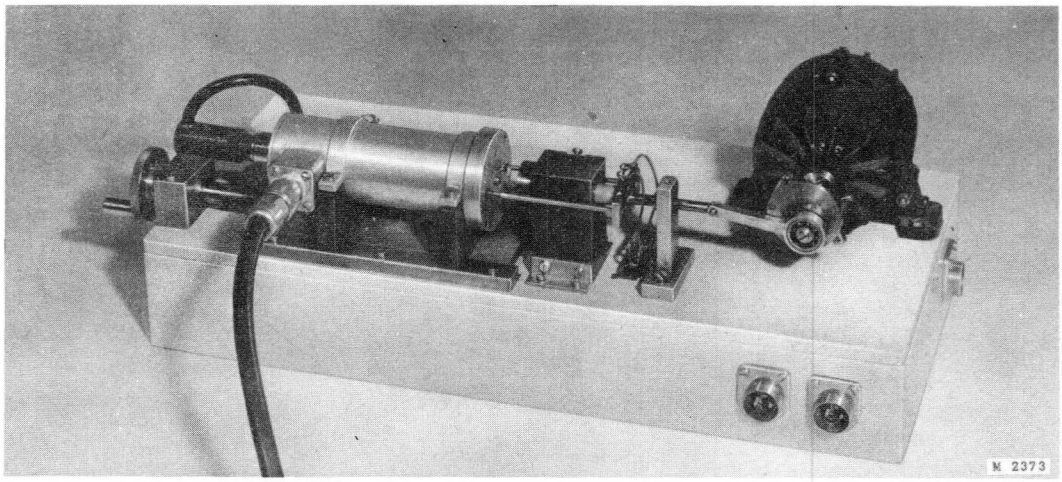

Fig.20. Assembled swept-frequency oscillator, showing the klystron oscillator on the left of the chassis, the encased pick-up mechanism in the middle, and the motor with eccentric at the right. At the extreme left the control knob for adjusting the centre frequency can be seen.

As mentioned above, the resonant circuit of the klystron oscillator is formed by a short-circuited coaxial pair. The short circuit is produced by a piston which is made non-contacting to keep the friction losses small. To ensure a good short-circuit over a wide frequency band, a sigma type of piston is used.

The piston is connected to two piston rods which are linked to the eccentric on the motor spindle by means of a junction bracket, a driving rod and a connecting rod. The pick-up coil is also fixed to the junction bracket and surrounded by a radially magnetised permanent magnet, similar to the construction of a moving-coil loudspeaker.

The eccentric is actually composed of two eccentrics fitting into each other, so that the eccentricity and thereby the frequency sweep of the oscillator can be varied. This construction is schematically represented in Fig.22.

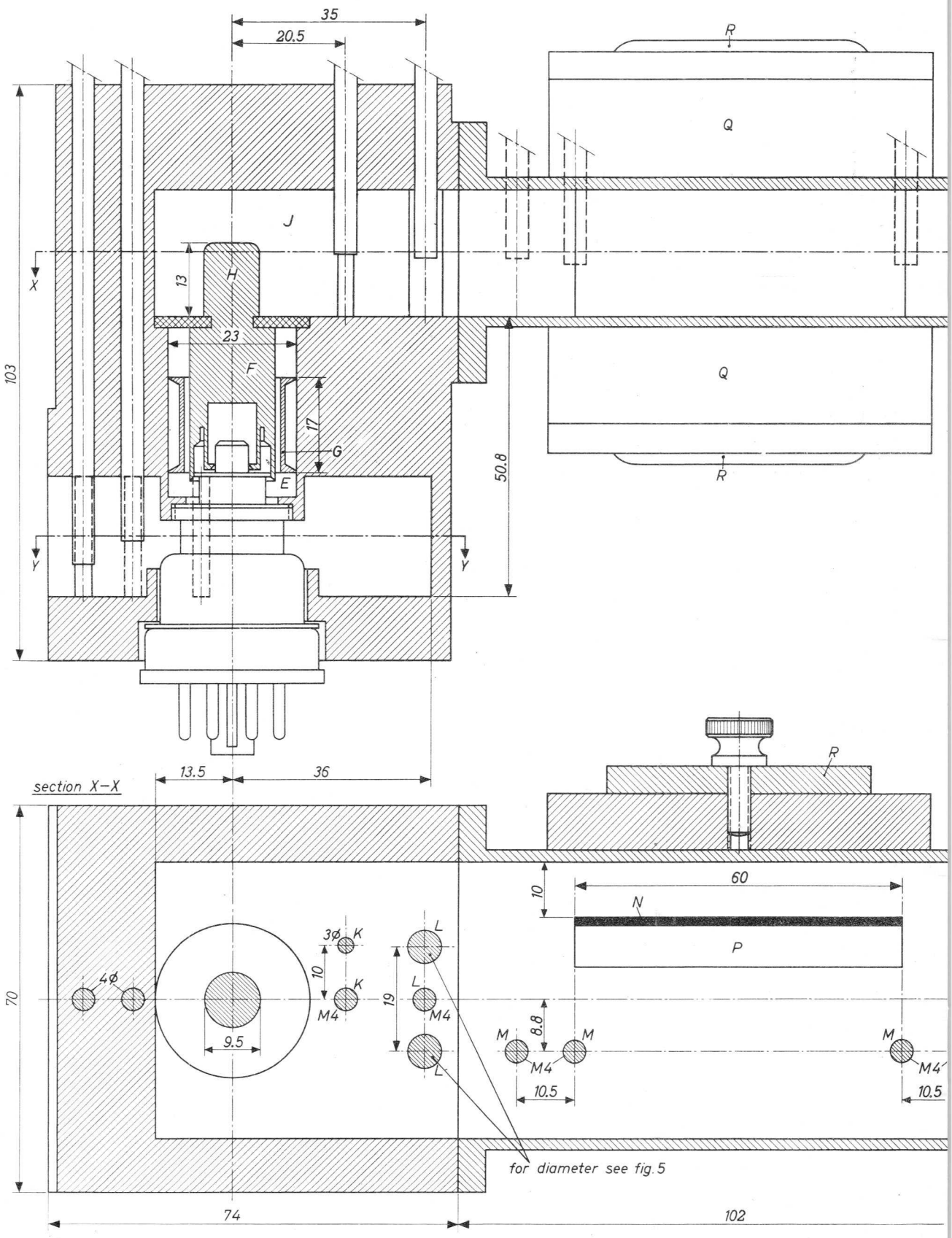
35
20.5
R
Q
J
X
13
H
23
F
17
G
E
103
50.8
Q
R
Y
Y
13.5
36
section X–X
R
60
10
N
P
3ø
K
10
K
M4
4ø
70
9.5
L
L
M4
19
L
M
8.8
M
M4
10.5
M
M4
10.5
for diameter see fig. 5
74
102

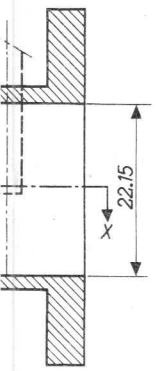

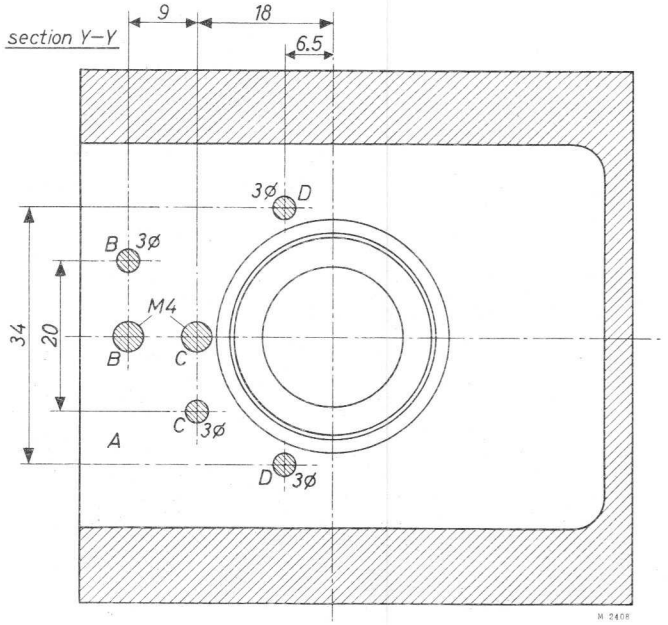

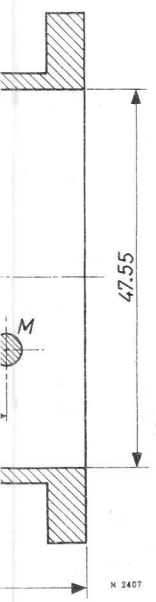

Slightly simplified cross-sections of the amplifier with interstage isolator with electrically essential dimensions in mm.

Legenda:

A Input waveguide.
B and *C* Matching transformer consisting of two matching strips and two tuning screws.
D Additional matching strips for the frequency range from 4000 to 4200 Mc/s.
E Anode cavity.
F Inner conductor of the $\lambda/4$ transformer.
G Piston, forming the outer conductor of the $\lambda/4$ transformer.
H Probe (coaxial to waveguide transition).
J Output waveguide.
K Variable susceptance, consisting of a matching strip and a tuning screw.
L Iris, consisting of two interchangeable matching strips and a tuning screw.
M Matching screws of the ferrite isolator.
N Ferroxcube slab.
P Quartz plate.
O Permanent magnets.
R Variable reluctance.

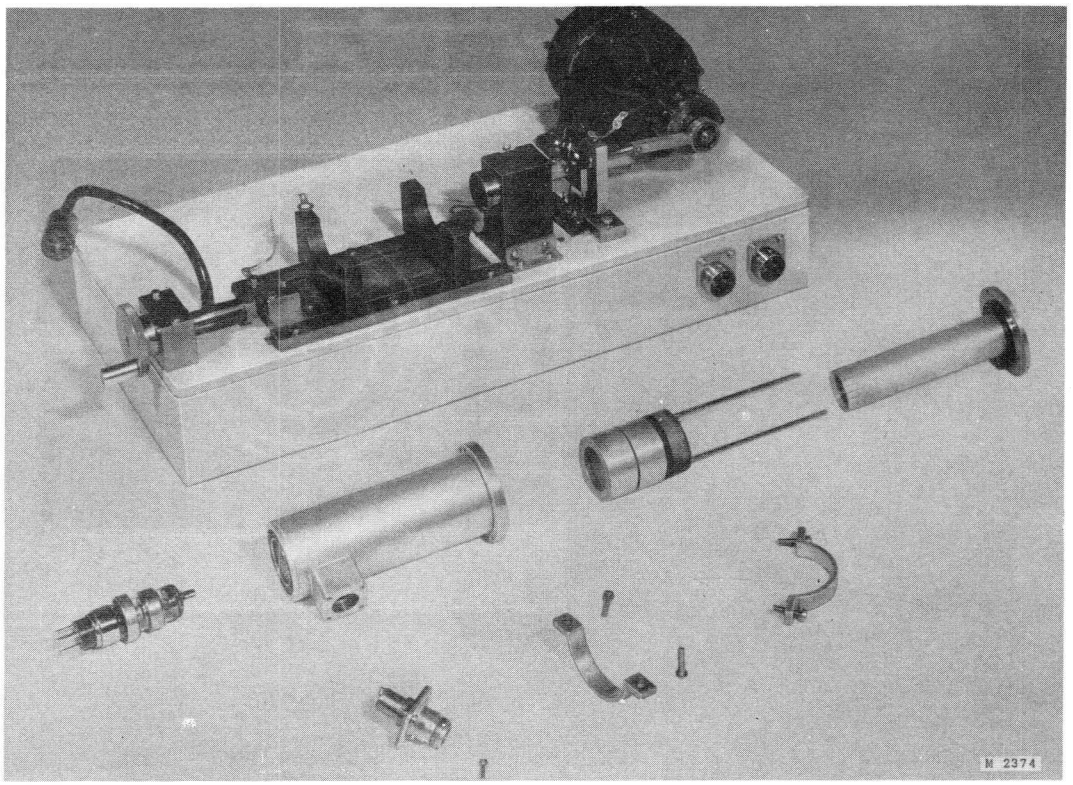

Fig.21. Partly dismounted swept-frequency oscillator. In the middle from left to right: reflex klystron, outer conductor, non-contacting sigma piston and inner conductor of the coaxial line. In the foreground: the coaxial output plug with coupling loop and the fixing brackets of the coaxial line.

The disc *A* is fixed to the motor spindle *B* and provided with an aperture in which the disc *C* can rotate around its axis *F*. The connecting rod *E* is linked by means of a ball bearing to the crank *D* on the disc *C*. During operation the latter is tightened in the disc *A*, so that, as a result of the rotation of the motor spindle *B* with its disc *A*, the crank *D* describes a circular movement with radius *BD*.

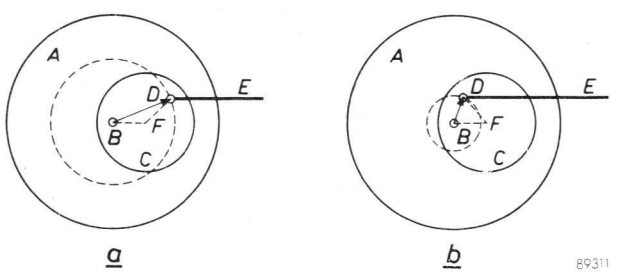

Fig.22. Basic principle of the adjustable eccentric. The eccentricity is greater in (a) than in (b) since the disc C occupies a different position in the disc *A*.

The degree of eccentricity can be adjusted by turning *C* with respect to *A*, this being achieved by means of a worm gear that can be locked by a screw.

The oscillator is mounted on a support that can be shifted in the longitudional direction with respect to the chassis; this is achieved by means of a threaded spindle. As a result of this displacement, the average electrical length of the transmission line is modified, and the centre frequency can thereby be adjusted.

The disc-shaped lead-ins of the grids of the klystron are connected to the inner and outer conductor respectively of the coaxial pair by means of resilient rings. The repeller connection of the tube is situated entirely within the hollow inner conductor, through which its supply voltage is applied.

The cathode and filament connections are established by means of a multiple plug and a flexible cable.

The R.F. power is taken inductively from the oscillator by means of a coupling loop. This loop is fixed to a plug which is connected to the coaxial pair leading to the test bench.

CIRCUIT DIAGRAM

Fig. 23 shows the complete circuit diagram, the various parts of which will be discussed in brief.

The following supply units are schematically indicated at the left of the circuit diagram:

(1) A 250 V stabilized supply unit for the anode and screen-grid voltages of the amplifying tubes.
(2) A 325 V stabilized supply unit for the resonator voltage of the klystron.
(3) A stabilized supply unit for an adjustable voltage of -30 V to -250 V for the repeller of the klystron.

The pick-up coil of the oscillator, which supplies an r.m.s. voltage of approximately 0.3 V, is connected to the control grid of the amplifying tube T_1. Its amplified alternating anode voltage, which is in anti-phase with the control-grid voltage, is applied to the integrating network consisting of two R-C elements connected in cascade. The component values are so chosen that the voltage across the capacitor C_5 leads 90° with respect to the anode voltage of T_1.

The phase shift is adjusted to its correct value by means of the variable resistor R_7. Part of the integrated voltage is applied to the first control grid of the gating tube T_5 (a heptode E 91 H) via the potentiometer R_{24}. Another part of the integrated voltage is applied to the grid of the left section of the double triode T_2 via the voltage divider R_8, R_9. The right triode section of this tube is d.c. coupled to the left section. The voltage at the anode or at the (unbypassed) cathode of the right triode section, depending on the phase relation in the horizontal deflection amplifier, is applied to the cathode-ray oscilloscope.

Part of the anode voltage of T_1 is amplified by T_3 and subsequently fed to the control grid of the pentode T_4. This voltage has a peak value of approximately 40 V, which results in the grid base of T_4 being far exceeded. The resistors R_{19} and R_{20} have been so chosen that the grid bias adjusts itself approximately to the cut-off point of the tube. No anode current will therefore flow during the negative half cycles, whereas during the positive half cycles the grid voltage is distorted to such an extent owing to the occurrence of grid current, that the anode voltage assumes a substantially square-wave form as shown in Fig. 24. This voltage is applied to the third grid of the gating tube T_5.

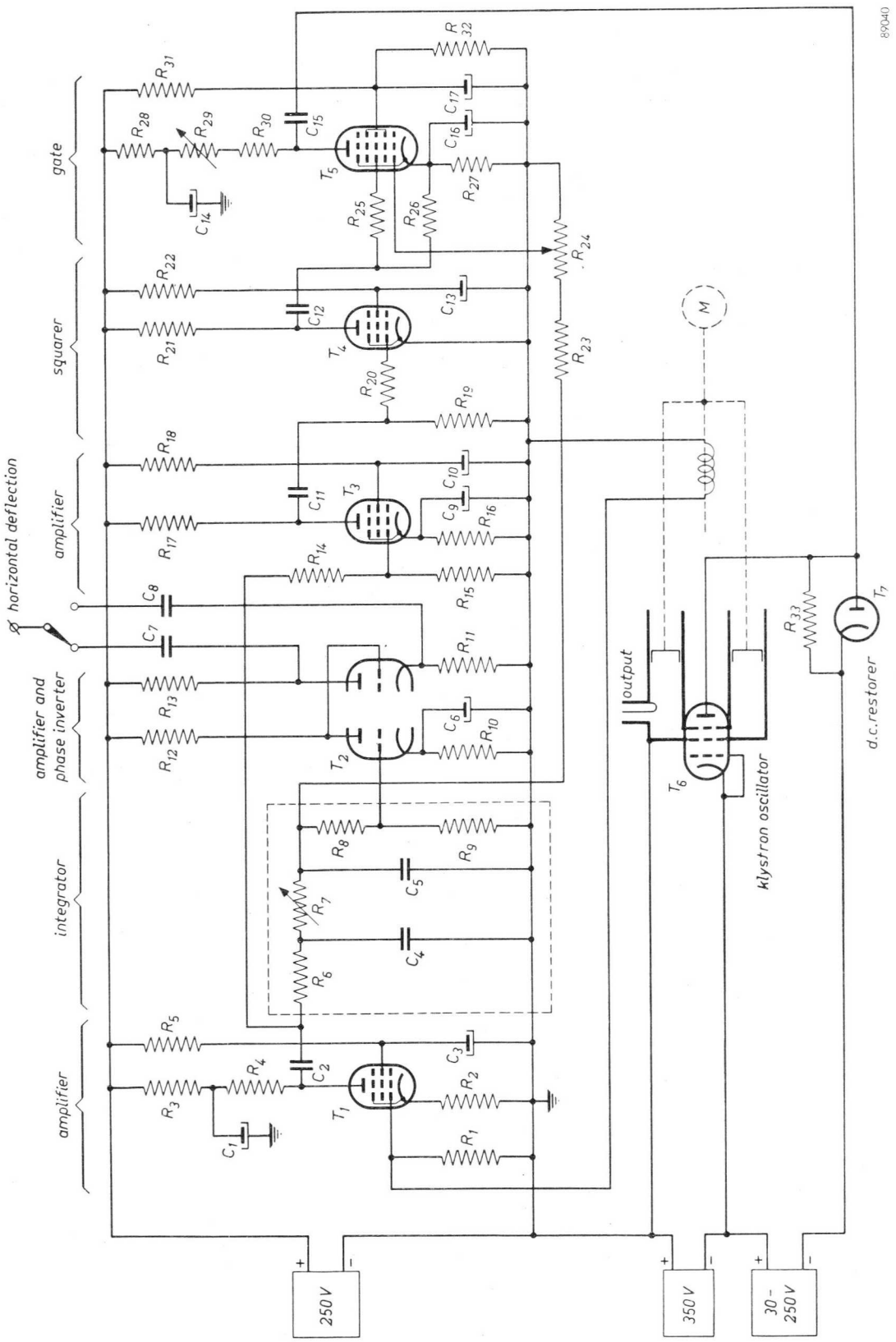

Fig.23. Diagram of the swept-frequency oscillator with its control circuits.

The anode voltage of T_5, which is represented in Fig. 19e, is applied in series with the direct voltage, to the repeller of the klystron. Since the anode voltage of T_5 has a direct voltage component, the blocking capacitor C_{15} has been provided, so that the negative supply voltage for the repeller need not be made very high. In order to ensure that the horizontal part of the voltage pulse is nevertheless kept at the desired direct voltage level of the repeller, the series resistor R_{33} is shunted by the diode T_7, which operates as a d.c. restorer.

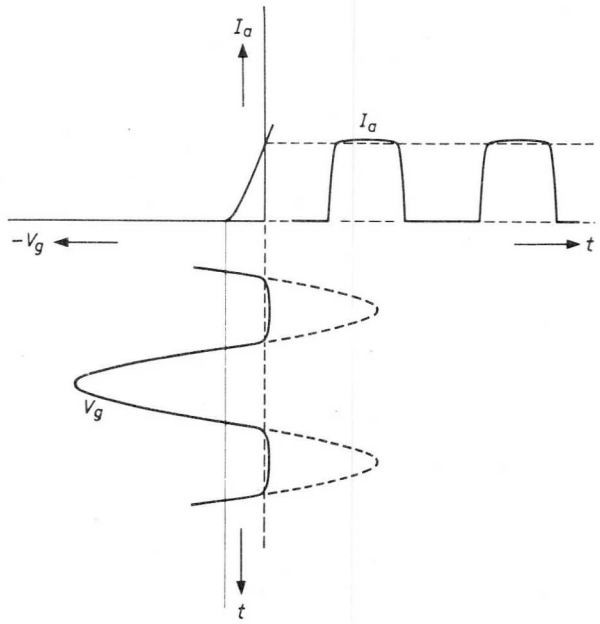

Fig. 24. Diagram illustrating the operation of the squarer.

CALIBRATION OF THE MEASURING SET-UP

The following parts of the measuring set-up should be adjusted and/or calibrated: (a) three ferrite isolators, (b) two detector mounts, (c) five resonant cavities, (d) two oscilloscopes.

There are two methods of adjusting the ferrite isolators; the first employs a standard signal generator, whilst for the second method an additional antenna isolator is needed.

The tuning of the resonant cavities should be carried out with the aid of a reference frequency, e.g. a standard signal generator or a calibrated wavemeter. The frequencies at which the cavities are tuned, are: f_0 - 125 Mc/s, f_0 - 25 Mc/s, f_0, f_0 + 25 Mc/s and f_0 + 125 Mc/s respectively, where f_0 is the centre frequency.

PARTS LIST (Fig. 23)

R_1 = 56 Ω, ½ W
R_2 = 1.2 kΩ, 1 W
R_3 = 10 kΩ, 1 W
R_4 = 220 kΩ, 1 W
R_5 = 1.2 MΩ, 1 W
R_6 = 470 kΩ, ½ W
R_7 = 1 MΩ, 1 W
R_8 = 1.8 MΩ, ½ W
R_9 = 390 kΩ, ½ W
R_{10} = 5.6 kΩ, 1 W
R_{11} = 560 kΩ, ½ W
R_{12} = 560 kΩ, ½ W
R_{13} = 560 kΩ, ½ W
R_{14} = 3.9 MΩ, ½ W
R_{15} = 270 kΩ, ½ W
R_{16} = 1.2 kΩ, 1 W
R_{17} = 47 kΩ, 1 W
R_{18} = 68 kΩ, 1 W
R_{19} = 1 MΩ, ½ W
R_{20} = 4.7 MΩ, ½ W
R_{21} = 47 kΩ, 1 W
R_{22} = 100 kΩ, 1 W
R_{23} = 1 MΩ, ½ W
R_{24} = 1 MΩ, 1 W
R_{25} = 470 kΩ, ½ W
R_{26} = 1 MΩ, ½ W
R_{27} = 220 Ω, 1 W
R_{28} = 12 kΩ, 1 W
R_{29} = 10 kΩ, 3 W
R_{30} = 18 kΩ, 1 W
R_{31} = 12 kΩ, 1 W
R_{32} = 560 kΩ, ½ W
R_{33} = 1 MΩ, ½ W
C_1 = 50 μF, 450 V
C_2 = 1 μF, 250 V
C_3 = 50 μF, 450 V
C_4 = 39 000 pF
C_5 = 56 000 pF
C_6 = 2 x 250 μF, 25 V
C_7 = 1 μF, 250 V
C_8 = 1 μF, 250 V
C_9 = 2 x 250 μF, 25 V
C_{10} = 50 μF, 450 V
C_{11} = 1 μF, 250 V
C_{12} = 1 μF, 250 V
C_{13} = 50 μF, 450 V
C_{14} = 50 μF, 450 V
C_{15} = 1 μF, 700 V
C_{16} = 2 x 250 μF, 25 V
C_{17} = 50 μF, 450 V
T_1 = E 80 F
T_2 = E 80 CC
T_3 = E 83 F
T_4 = E 83 F
T_5 = E 91 H
T_6 = 6 BL 6
T_7 = EA 50

For rapidly judging the performance of the amplifier and the ferrite isolators the screens of the oscilloscopes can be marked with some reference lines (see Figs 25 and 26).

The modulus of the reflection coefficient is indicated on Osc_1 in the form of the V.S.W.R. occurring in the waveguide. The screen of this oscilloscope should be marked with reference lines according to a V.S.W.R. of 1, 2, 2.3 and 2.6, which correspond to power losses of 0, 0.5, 0.75 and 1 dB respectively. These reference lines can be obtained with the aid of a calibrated standing-wave introducer.

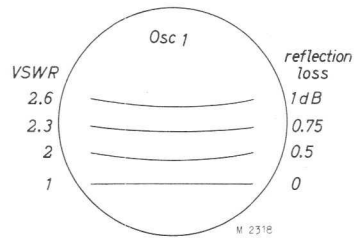

Fig.25. Reference lines on the screen of oscilloscope Osc_1 (reflection).

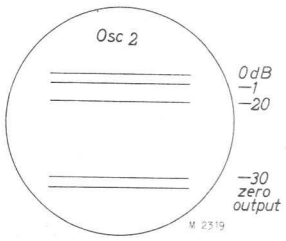

Fig.26. Reference lines on the screen of oscilloscope Osc_2 (response).

When the entire power passed by the second directional coupler is transferred to the detector at the end of the test bench, a line is produced on the screen of Osc_2 corresponding to a gain of 0 dB. With switch S in position a, the amplification of $Ampl_2$ is so adjusted that this line coincides with the reference line of 0 dB. The reference line of zero output coincides with the line traced on the screen during fly-back of the beam.

Three other reference lines corresponding to -1, -20 and -30 dB, can been obtained with the aid of the calibrated attenuators. Due to the low sensitivity in the case of -20 and -30 dB, the additional amplifier $Ampl_3$ is switched on (S in position f) when these attenuations are considered (see Fig.15).

ADJUSTMENT AND TEST OF THE FERRITE ISOLATORS

THE INTERSTAGE ISOLATOR

First the isolator is adjusted for maximum reverse attenuation. It is therefore so inserted in the test set-up that the arrow indicating the direction "pass", points towards the generator. Switch S is set to position f.

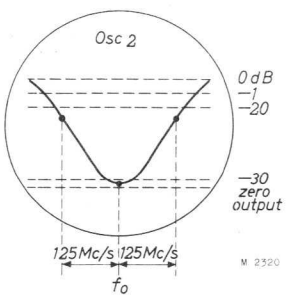

Fig.27. Check on the reverse attenuation and the bandwidth of the ferrite isolator as indicated on Osc_2.

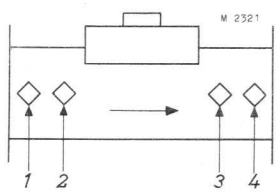

Fig.28. Indication of the control screws of the ferrite isolator.

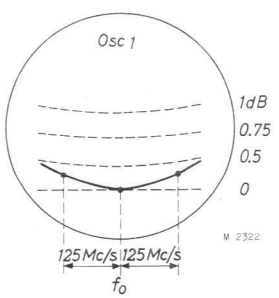

Fig.29. Picture displayed on Osc_1 when the ferrite isolator is correctly matched.

Now the magnetic series resistance is so adjusted that at the centre frequency the transmitted signal is at a minimum. The correct reverse attenuation and the correct bandwidth can be checked as follows: on Osc_2 the marking spot corresponding to f_0 must be below the reference line of -30 dB, whilst the marking spots corresponding to $f_0 \pm 125$ Mc/s must be below the reference line of -20 dB (see Fig.27).

Subsequently the correct matching of the input sides can be brought about. For this purpose the isolator is reversed (arrow pointing towards the detector) and the setting screws *1* and *2* (Fig.28) are adjusted for minimum reflection at the centre frequency. On Osc_1 a graph is seen analogous to that of Fig.29. The forward attenuation can be checked by making sure that, with switch *S* in position *a*, the entire graph on Osc_2 lies above the reference line of -1 dB.

Finally, the isolator is reversed again, and the setting screws *3* and *4* are adjusted for minimum reflection.

THE ANTENNA ISOLATOR

The procedure for adjusting the antenna isolator is identical to that of the interstage isolator. Since this long isolator gives a very weak reflection, it is not always easy to check the V.S.W.R.

ADJUSTMENT AND TEST OF THE AMPLIFIER

Together with the ferrite isolator and connector, the amplifier is inserted in the test bench with the input side pointing to the generator.

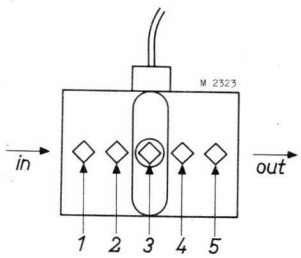

Fig.30. Indication of the control screws of the amplifier.

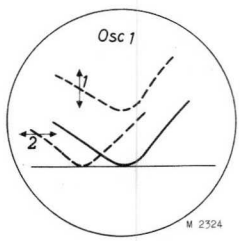

Fig.31. Effect of turning the screws *1* and *2*.

First the input impedance of the amplifier is adjusted for minimum reflection with the anode circuit shortcircuited for R.F., which is achieved by tuning the anode cavity to its lowest resonant frequency (setting screw *3* (Fig.30) turned clockwise to its end position). The matching of the input is accomplished with the setting screws *1* and *2* (Fig.30). By turning screw *1*, mainly the real part of the input impedance is varied, whereas the resonant frequency is influenced by screw *2*. The effect of turning these screws can be seen on Osc_1 (see Fig.31).

Subsequently the amplifier is adjusted for maximum flatness of its response curve with the aid of the setting screws *3*, *4* and *5*. After this, the matching of the input side, which is affected by the manipulation at the anode side, is readjusted [1]).

[1]) It is also possible to omit the readjustment of the cathode circuit; it is true, that a small reflection then occurs at the input, but the bandwidth of the cathode circuit will be slightly greater.

A check on the correct response curve reveals that on Osc_2 a graph is seen similar to Fig.32, in which the marking spots of f_0 ± 25 Mc/s indicate whether the 0.1 dB bandwidth is larger than 50 Mc/s or not. The 0.5 dB bandwidth of the cathode side should also be larger than 50 Mc/s, which can be seen on Osc_1 (see Fig.33). The bandwidth of the input side depends to a large extent on the tube used and on the frequency.

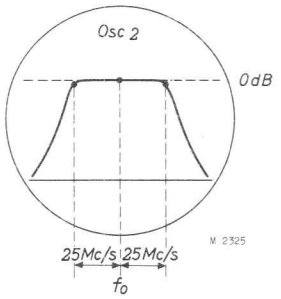

Fig.32. Check on the flatness and the bandwidth of the response curve as indicated on Osc_2.

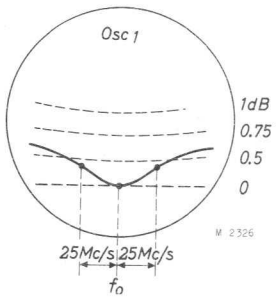

Fig.33. Indication of the correct reflection of the input side of the amplifier as displayed on Osc_1.

With the aid of the calibrated attenuators the signal at the detector is so adjusted that on Osc_2 the maximum value of the response curve coincides with the reference line of 0 dB. The power gain of the amplifier (minus losses due to the ferrite isolator) can then be read directly on the attenuators.

GENERAL DATA OF THE EC 56 AND EC 57

Heating:	indirect by a.c. or d.c.	
	Parallel supply only.	
	Heater voltage	V_f = 6.3 V [1]
	Heater current	I_f = 0.65 A
Capacitances:	Inter electrode capacitances (V_f = 6.3 V; I_k = 0)	
	Anode-to-grid	C_{ag} = 1.6 pF
	Anode-to-cathode	C_{ak} = 40 mpF
	Grid-to-cathode	C_{gk} = 3.3 pF

The maximum heater-to-cathode current is 100 μA at a heater-to-cathode voltage of 50 V and a heater voltage of 6.3 V.

ELECTRODE ARRANGEMENT, CONNECTIONS AND DIMENSIONS

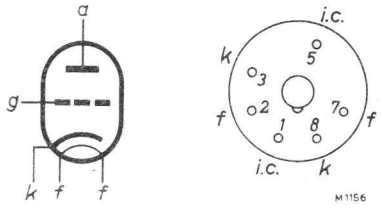

Fig.35. Electrode arrangement and base connections.

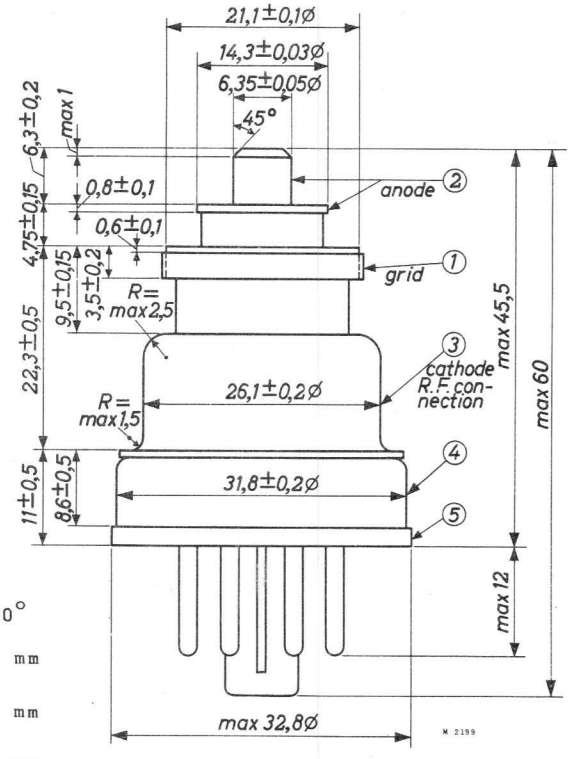

Data of thread of the grid disc:
32 turns per inch; thread angle 60°

minor diameter	: 21.22 $^{+\ 0}_{-\ 0.15}$	mm
major diameter	: 22.2 $^{+\ 0}_{-\ 0.15}$	mm
effective diameter	: 21.68 $^{+\ 0}_{-\ 0.09}$	mm

Fig.36. Dimensional drawing [2] and electrode connections (dimensions in mm).

For footnotes [1] and [2] see following page.

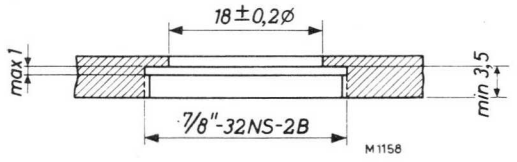

Fig.37. Recommended mount [2]) (dimensions in mm).

Data of thread:

32 turns per inch; thread angle 60°

minor diameter : $21.51\ ^{+\ 0}_{-\ 0.15}$ mm

major diameter : min.22.23 mm

effective diameter : $21.83\ ^{+\ 0}_{-\ 0.12}$ mm

CAUTION

Special attention should be paid to the mounting of the EC 56 and EC 57 in those cases where they are used in transportable equipment. Shocks, especially in a direction perpendicular to the axis of the tube, should be avoided.

The maximum torque which may be exerted on the anode disc with respect to the base is 0.23 kgm (20 lbs inch).

---

[1]) In order to ensure a long tube life the maximum variation of the heater voltage should not exceed ± 2% (absolute limits).

[2]) The following points should be considered with respect to the maximum eccentricities, referring to the figures 1 to 5 within the small circles in Fig.36.

(1) The eccentricities are given with respect to the axis of the threaded hole, shown in Fig.37, the grid disc of the tube being screwed firmly against the R.F. contacting surface of the flange (with inner diameter of 18 mm).

(2) Maximum eccentricity of the axis of the anode 0.15 mm.

(3) The distance between the surface of the cylindrical part of the cathode R.F.connection and the axis of the threaded hole, specified in Fig.37, is 12.85 mm minimum and 13.25 mm maximum.

(4) The tolerance of the eccentricity of the axis of the base is such that this base fits into a hole with a diameter of 32.5 mm, provided this hole is correctly centred with respect to the axis of the hole specified in Fig.37.

(5) The tolerance of the eccentricity of the axis of the base flange is such that this base flange fits into a hole with a diameter of 33.5 mm, provided this hole is correctly centred with respect to the axis of the hole specified in Fig.37.

TECHNICAL DATA OF THE EC 56

TYPICAL CHARACTERISTICS

			nom.	min.	max.	
Anode voltage	V_a	=	180	-	-	V
Anode current	I_a	=	30	-	-	mA
Grid voltage	V_g	=	-2.8	-4.0	-1.8	V
Mutual conductance	S	=	17	13.5	-	mA/V
Amplification factor	μ	=	43	33	52	

OPERATING CONDITIONS AS GROUNDED GRID AMPLIFIER AT 4000 Mc/s

Anode supply voltage	V_{ba}	=	200 V
Grid supply voltage	V_{bg}	=	+20 V
Cathode bias resistor	R_k	=	max. 1 kΩ [3]
Anode current	I_a	=	30 mA
Bandwidth (0.1 dB down)	B	=	50 Mc/s [4]
Power gain at 1 mW output power	G	=	12 dB (min. 10 dB)
Output power at 6 dB power gain (V_f = 6.3 V)	W_o	=	0.5 W (min. 0.35 W)

MAXIMUM RATINGS (absolute maxima)

Anode voltage at zero anode current	V_{a0}	=	500 V
Anode voltage	V_a	=	300 V
Anode dissipation	W_a	=	10 W
Cathode current	I_k	=	35 mA
Grid current	I_g	=	10 mA
Driving power (grounded grid)	W_{dr}	=	0.5 W
Direct grid voltage (positive)	V_g	=	0 V
Direct grid voltage (negative)	V_g	=	-50 V
Heater-to-cathode voltage	V_{kf}	=	50 V
External resistance between cathode and heater	R_{kf}	=	20 kΩ
External resistance between grid and cathode	R_{gk}	=	25 kΩ
Anode seal temperature	t_a	=	150 °C [5]
Grid seal temperature	t_g	=	75 °C [5]
Cathode seal temperature	t_k	=	75 °C [5]

---

[3]) A variable resistor should be used for this purpose to adjust the anode current to the required value. (See the recommended d.c. circuit shown in the adjacent figure.)

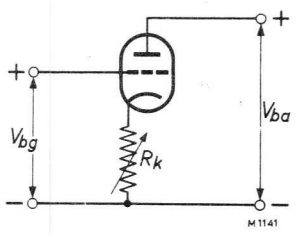

[4]) The quoted value is the bandwidth between the 0.1 dB points of the flattened response curve depicted in Fig.1 (see p.6). This shape of response curve occurs in the microwave amplifier discussed in this Bulletin in which a transitionally coupled band-pass filter is incorporated in the anode circuit.

[5]) Low velocity air circulation may be required. In the amplifier discussed in this Bulletin, 6 to 10 litres of cooling air per minute are sufficient.

TECHNICAL DATA OF THE EC 57

TYPICAL CHARACTERISTICS			nom.	min.	max.	nom.
Anode voltage	V_a	=	180	-	-	180 V
Anode current	I_a	=	30	-	-	60 mA
Grid voltage	V_g	=	-2.8	-4.0	-1.8	-1.6 V
Mutual conductance	S	=	17	13.5	-	19 mA/V
Amplification factor	μ	=	43	33	52	43

OPERATING CONDITIONS AS GROUNDED GRID AMPLIFIER AT 4000 Mc/s

Anode supply voltage	V_{ba}	=	200 V
Grid supply voltage	V_{bg}	=	+20 V
Cathode bias resistor	R_k	=	max. 500 Ω [3]
Anode current	I_a	=	60 mA
Bandwidth (0.1 dB down)	B	=	50 Mc/s [4]
Output power at 8 dB power gain (V_f = 6.3 V)	W_o	=	1.8 W (min. 1.5 W)

MAXIMUM RATINGS (absolute maxima)

Anode voltage at zero anode current	V_{ao}	=	500 V
Anode voltage	V_a	=	300 V
Anode dissipation	W_a	=	10 W
Cathode current	I_k	=	70 mA
Grid current	I_g	=	10 mA
Driving power (grounded grid)	W_{dr}	=	1 W
Direct grid voltage (positive)	V_g	=	0 V
Direct grid voltage (negative)	V_g	=	-50 V
Heater to cathode voltage	V_{kf}	=	50 V
External resistance between cathode and heater	R_{kf}	=	20 kΩ
External resistance between grid and cathode	R_{gk}	=	25 kΩ
Anode seal temperature	t_a	=	150 °C [5]
Grid seal temperature	t_g	=	75 °C [5]
Cathode seal temperature	t_k	=	75 °C [5]

CHARACTERISTICS

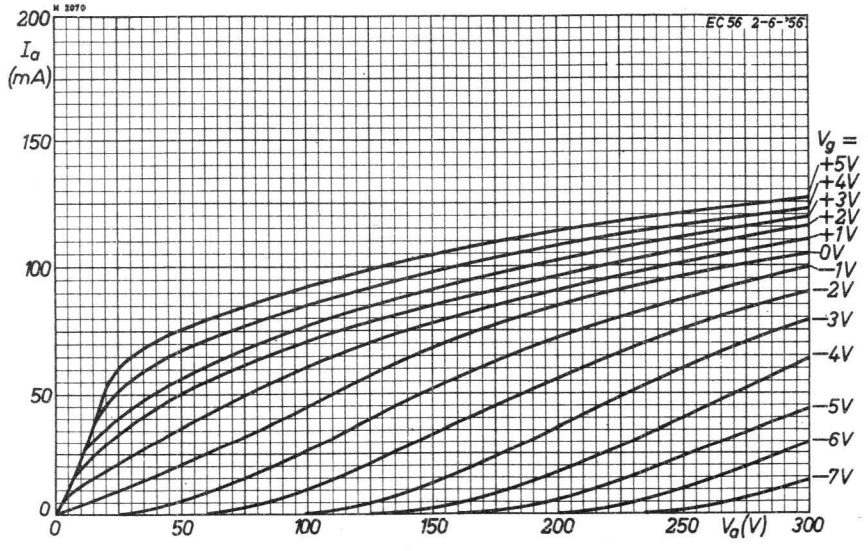

Fig.38. I_a/V_a characteristics of the EC 56 with the grid voltage (V_g) as parameter.

For footnotes [3], [4] and [5] see preceding page.

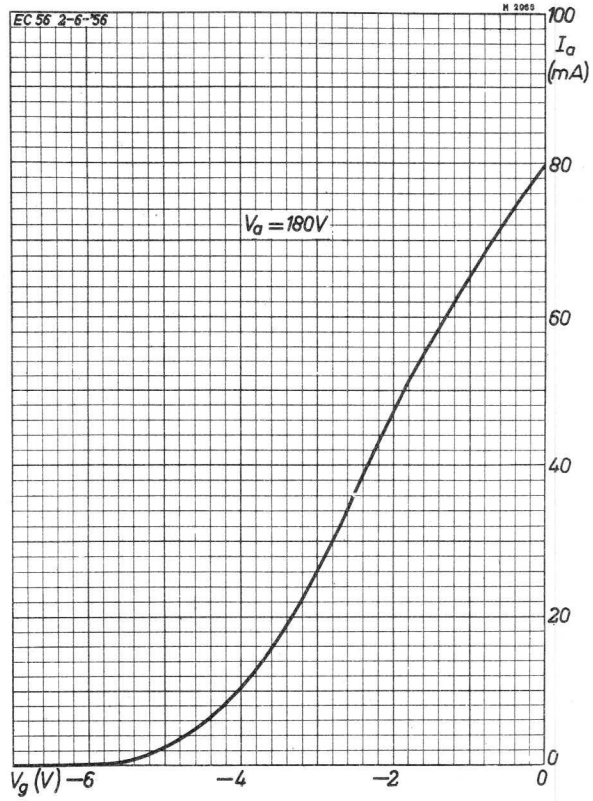

Fig.39. I_a/V_g characteristic of the EC 56 at an anode voltage of 180 V.

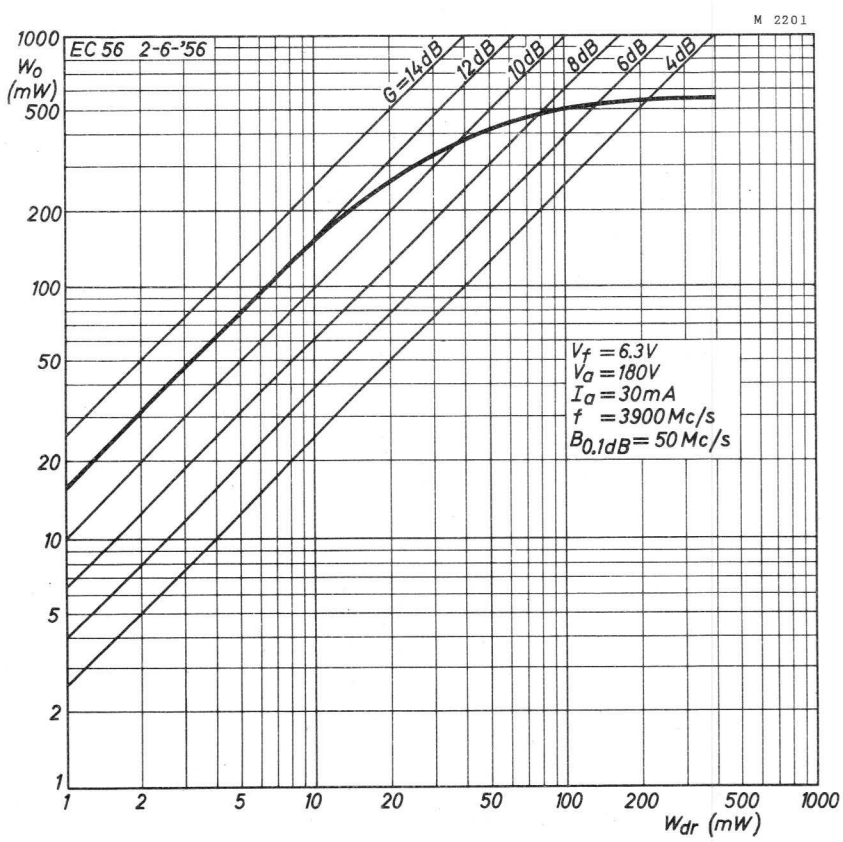

Fig.40. Output power (W_o) of the EC 56 as a function of the driving power (W_{dr}) with lines of constant power gain (G); (f = 3900 Mc/s. $B_{0.1\ dB}$ = 50 Mc/s, V_a = 180 V, I_a = 30 mA).

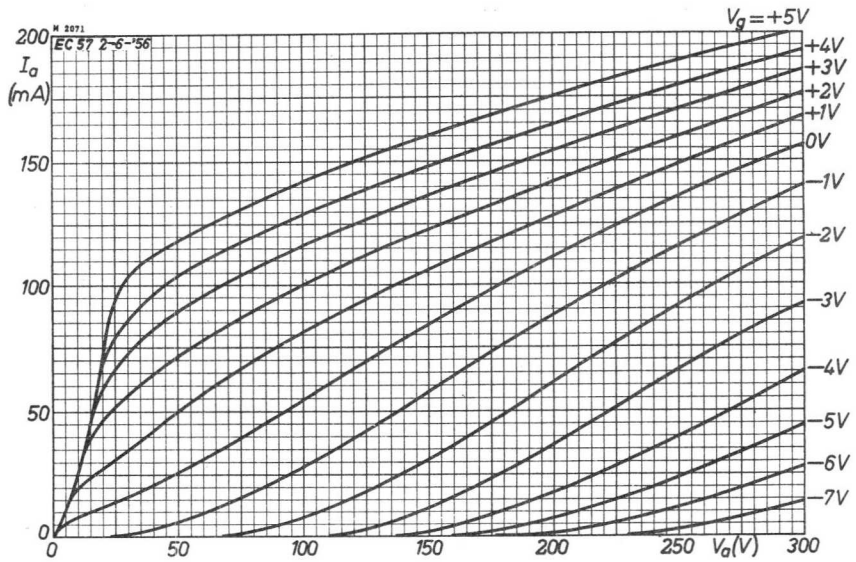

Fig.41. I_a/V_a characteristics of the EC 57 with the grid voltage (V_g) as parameter.

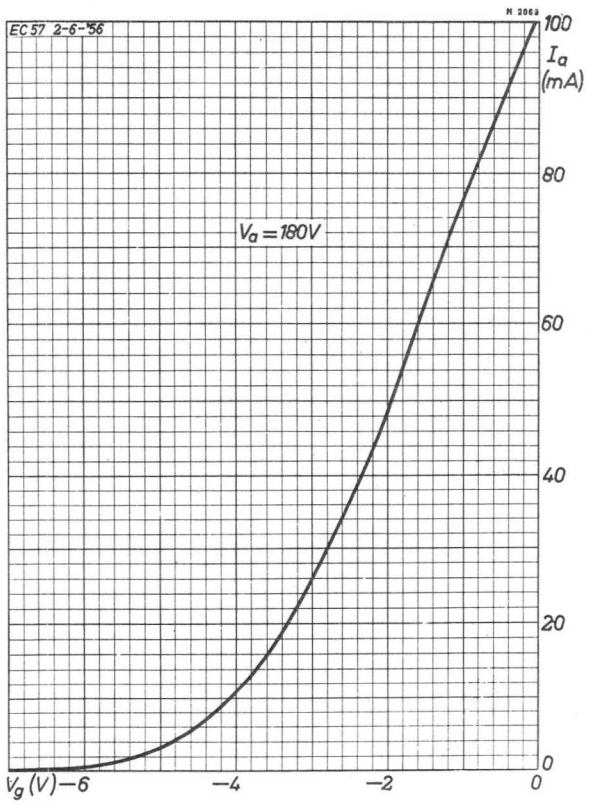

Fig.42. I_a/V_g characteristic of the EC 57 at an anode voltage of 180 V.

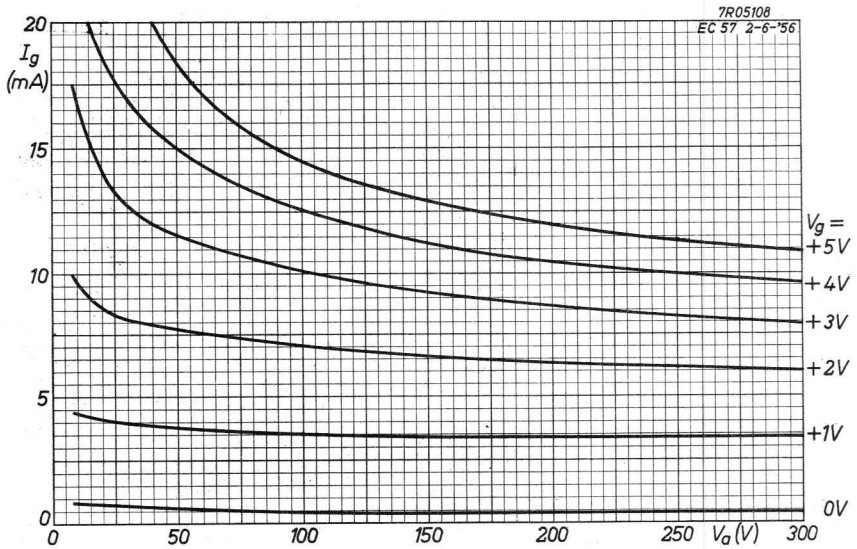

Fig.43. I_g/V_a characteristics of the EC 57 with the grid voltage (V_g) as parameter.

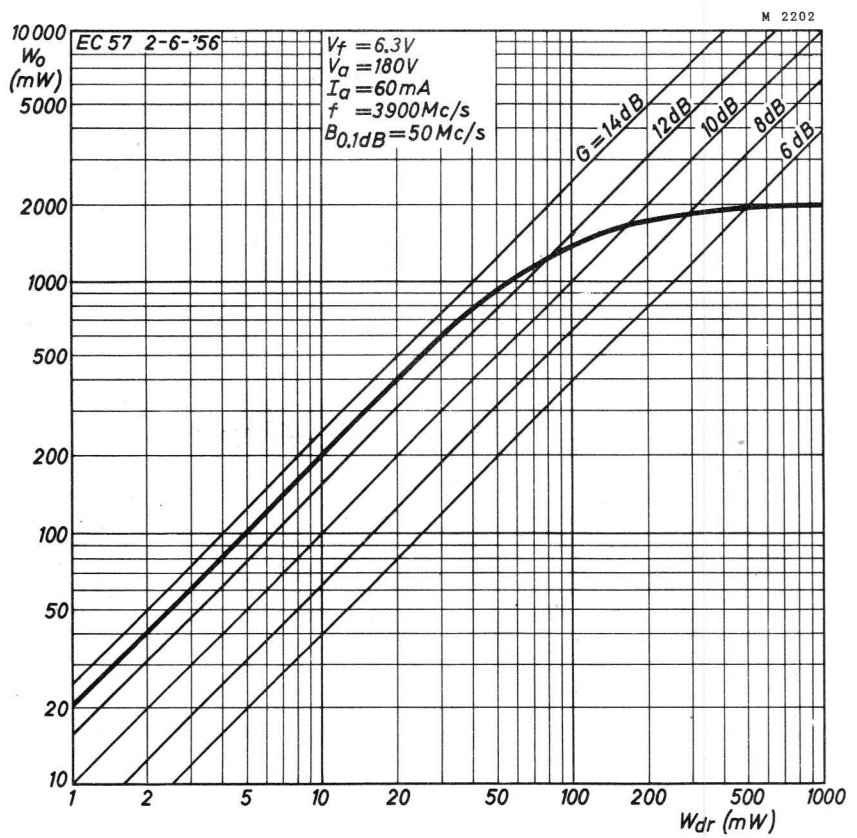

Fig.44. Output power (W_o) of the EC 57 as a function of the driving power (W_{dr}) with lines of constant power gain (G): (f = 3900 Mc/s. $B_{0.1\ dB}$ = 50 Mc/s. V_a = 180 V. I_a = 60 mA).

APPENDICES

I. Analysis of the Anode Circuit

It is shown in this Appendix how the anode circuit of the amplifier is designed to obtain the required flat response curve.

The first resonant circuit of the complete anode circuit is formed by the cavity that surrounds the anode part of the EC 56, whilst the second resonant circuit is formed by an iris, the two circuits being coupled by a waveguide section. To separate the iris from the following stage (i.e. the cathode circuit of the following tube), which is essential because the iris is very sensitive to detuning, the latter should be followed by a unidirectional coupler. The further advantages of this unidirectional coupler are discussed in Section 7.

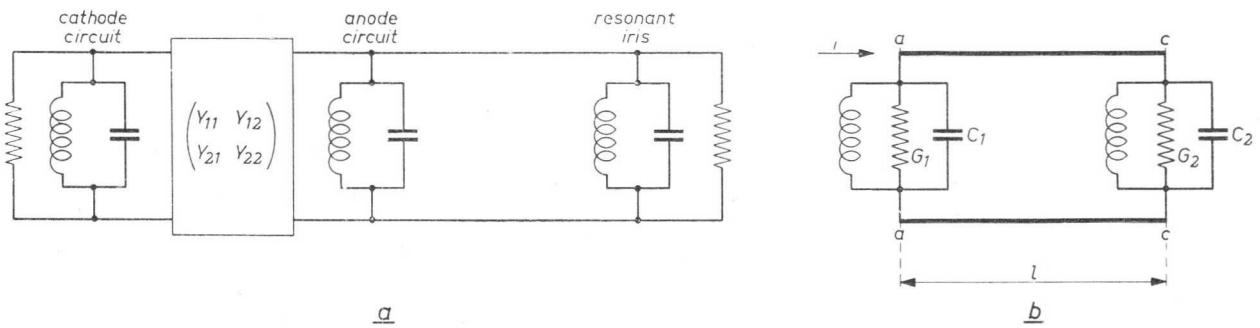

Fig.45. (a) Schematic representation of the total amplifier. (b) Equivalent circuit by means of which the behaviour of the total circuit can be described.

The entire amplifier comprises three resonant circuits, viz. the cathode circuit, the resonant circuit around the anode and the resonant iris (see Fig.45a). Due to the heavy loading of the tube itself the bandwidth of the cathode circuit is large. Since the influence of the tube impedance on the anode circuit is small as a result of the heavy loading of the waveguide, the behaviour of the entire circuit can be described with the aid of the equivalent circuit of Fig.45b. The bandwidth of the cathode side being large, it may be assumed that the current as a function of the frequency is constant in the frequency range considered.

The anode admittances and the anode current are referred to the waveguide. Seen from the waveguide, from the load towards the amplifier, an admittance is seen the value of which depends on the reference plane in the waveguide. The plane at which a parallel tuned resonant circuit is seen is denoted by aa in Fig.45b. The distance between the resonant iris and this plane is indicated by the length l. The admittance of the first resonant circuit is denoted by Y_1 and that of the second resonant circuit, i.e. the resonant iris, by Y_2.

1. THE EXPRESSION FOR THE TRANSFER ADMITTANCE

According to eq.(2.5) of an article published in Electronic Applications Vol.16, p.81, 1955/56 (No.3) *), the transfer admittance of the total network is given by the expression:

$$-Y_{21}Y_{tr} = \Delta Y, \tag{1.1}$$

where ΔY is the determinant of the total network. The admittance matrix of a waveguide of length l is given by:

$$(y) = \begin{pmatrix} -\dfrac{jY_0}{\tan \beta l} & +\dfrac{jY_0}{\sin \beta l} \\ +\dfrac{jY_0}{\sin \beta l} & -\dfrac{jY_0}{\tan \beta l} \end{pmatrix},$$

where Y_0 denotes the surge impedance, $\beta = 2\pi/\lambda$ and l represents the length of the waveguide section. At $l = \lambda/4$ the admittance matrix is:

$$(y)_{\lambda/4} = \begin{pmatrix} 0 & jY_0 \\ jY_0 & 0 \end{pmatrix},$$

and eq (1.1) becomes:

$$-jY_0Y_{tr} = Y_0^2 + Y_IY_{II}, \tag{1.2}$$

where $Y_I = Y_{11} + Y_1$ and $Y_{II} = Y_{22} + Y_2$. In the case considered $Y_{11} = 0$ and $Y_{22} = 0$, so that $Y_I = Y_1$ and $Y_{II} = Y_2$.
Introduction of the parameters: x, r, l_1 and l_2 (see p.83 of Article I) gives:

$$-jY_0Y_{tr} = Y_0^2 + G_1G_2\left\{1 - l_1l_2 + \left(\frac{l_2}{\sqrt{r}} + l_1\sqrt{r}\right)x - x^2 - j(l_1 + l_2) + j\left(\sqrt{r} + \frac{1}{\sqrt{r}}\right)x\right\}, \tag{1.3}$$

where

$$x = \left(\frac{\omega}{\omega_m} - \frac{\omega_m}{\omega}\right)\sqrt{Q_1Q_2} = \beta \mid \overline{Q_1Q_2},$$

$$r = Q_2/Q_1, \qquad l_1 = 2p_1/B_1 \quad \text{and} \quad l_2 = 2p_2/B_2.$$

If the quality factor Q_1 of the first circuit is high, the value of r will be small, and when Q_1 approaches infinity the expression for the transfer admittance becomes:

$$-jY_0Y_{tr} = Y_0^2 - 4p_1p_2C_1C_2 + 2G_2C_1(p_1 + p_2)x' - \\ - G_2^2\frac{C_1}{C_2}x'^2 - j2p_1G_2C_1 + jG_2^2\frac{C_1}{C_2}x', \tag{1.4}$$

where $x' = x\sqrt{r}$ **).

*) Transfer Properties of a Network consisting of two Resonant Circuits coupled by a Fourpole. This Article will be referred to as Article I.

**) See Electr.Appl. Vol.16, p.112, 1955/56 (No.3).

In the EC 56 grounded-grid amplifier discussed in this Appendix the value of r is roughly 7, so that eq.(1.4) can be applied with reasonable approximation. In analogy with eq.(3.11) of Article I, this equation can be written in the general form:

$$\boxed{\bar{N} = a + bx' + cx'^2 + jd + jex'.} \qquad (1.5)$$

2. THE CONDITION FOR A SYMMETRICAL RESPONSE CURVE

For a symmetrical response curve to be obtained the condition $b = 0$ and $d = 0$ must be satisfied (see eq.(5.1) of Article I). This condition implies, according to eq.(1.4), that:

$$b = 2G_2C_1(p_1 + p_2) = 0 \quad \text{and} \quad d = -2p_1G_2C_1 = 0. \qquad (2.1)$$

Consequently, both p_1 and p_2 must be zero to ensure a symmetrical response curve, in other words the two resonant circuits must both be tuned to the desired frequency.

3. THE CONDITION FOR A FLAT RESPONSE CURVE

Since the response curve is assumed to be symmetrical,

$$-jY_0Y_{tr} = Y_0^2 - G_2^2 \cdot \frac{C_1}{C_2} x'^2 + jG_2^2 \cdot \frac{C_1}{C_2} x', \qquad (3.1)$$

which, in analogy with eq.(6.1) of Article I, may be written:

$$N = a + cx'^2 + jex'. \qquad (3.1a)$$

In Section 6.2 of Article I it is shown that the flatness of the response curve is a maximum if $a = -e^2/2c$, which in the case under consideration amounts to:

$$Y_0^2 = \frac{G_2^2C_1}{2C_2}, \quad \text{or} \quad \frac{Y^2}{G_2^2} \cdot \frac{C_2}{C_1} = \frac{1}{2}, \qquad (3.2)$$

where Y_0 = surge admittance of the coupling waveguide section,
G_2 = conductance of the second resonant circuit,
C_1 = reflected anode capacitance,
C_2 = capacitance of the second resonant circuit.

4. THE 0.1 dB BANDWIDTH OF THE CIRCUIT

It is shown elsewhere *) that in the case of transitional coupling (flat response curve) the 0.1 dB bandwidth is given by:

$$B_{0.1\text{dB}} = 0.39 \sqrt{-\frac{a}{c}} \cdot B_2$$

(cf. Section 9.2, p.91 of Article I). At the condition imposed by eq (3.2), $\sqrt{-a/c}$ becomes $1/\sqrt{2}$; hence:

$$B_{0.1\text{dB}} = 0.276\, B_2. \qquad (4.1)$$

---

*) See Electr.Appl. Vol.16 p.112 1955/56 (No.3).

5. THE POSSIBILITIES OF RENDERING THE RESPONSE CURVE FLAT

The condition imposed by eq (3.2) is not generally fulfilled, but if one of the quantities involved, i.e. Y_0, C_1, C_2 or G_2 can be adjusted, a flat response curve can be obtained.

The possibility of adjusting each of these quantities will now be investigated, it being assumed that the length of the line is $\lambda/4$.

5.1. ADJUSTMENT OF Y_0

If the surge admittance of the coupling waveguide is made variable, for example by the changing of its dimensions, the value of Y_0 can be adjusted in such a way that eq.(3.2) holds. Since the bandwidth B_2 remains the same, the 0.1 dB bandwidth will depend only on the bandwidth of the resonant iris.

The adjustment of the surge admittance of the coupling waveguide involves mechanical difficulties, however.

5.2. ADJUSTMENT OF C_2

The resonant iris is constructed as a circuit with two inductive posts and one variable capacitive post. If the inductance is decreased and the capacitance increased simultaneously, the resonant frequency will remain unchanged, but C_2 is increased, which results in a decrease of the bandwidth since the damping caused by the load is not influenced. It is thus possible to obtain a flat response curve by adjusting C_2 in this way.

According to eq.(4.1) the 0.1 dB bandwidth is given by:

$$B_{0.1\,\mathrm{dB}} = 0.276\, B_2 = 0.276\, \frac{G_2}{C_2}.$$

From eq.(3.2):

$$C_2 = \frac{G_2^2}{2Y_0^2} \cdot C_1 = kC_1,$$

$k = G_2^2/2Y_0^2$ being constant in this case. The 0.1 dB bandwidth thus becomes:

$$B_{0.1\,\mathrm{dB}} = \frac{0.276}{k}\, G_2 \cdot \frac{1}{C_1} = \text{constant} \cdot \frac{1}{C_1},$$

in other words the 0.1 dB bandwidth depends on the reflected anode capacitance. This method also has the drawback of involving mechanical difficulties.

5.3. ADJUSTMENT OF G_2

If the waveguide is provided with a variable admittance Y at a distance $\lambda/8$ from the resonant iris (see Fig.46), the damping G_2

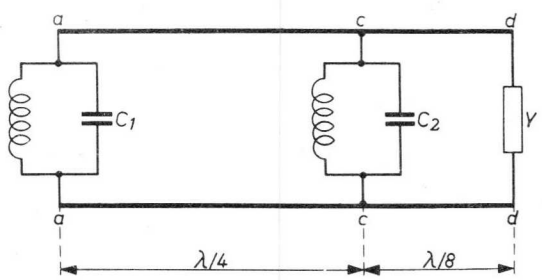

Fig.46. Waveguide provided with a variable admittance Y, at a distance $\lambda/8$ from the resonant iris, for adjusting the damping G_2.

of the latter can be adjusted. This can easily be seen from the Smith chart shown in Fig.47.

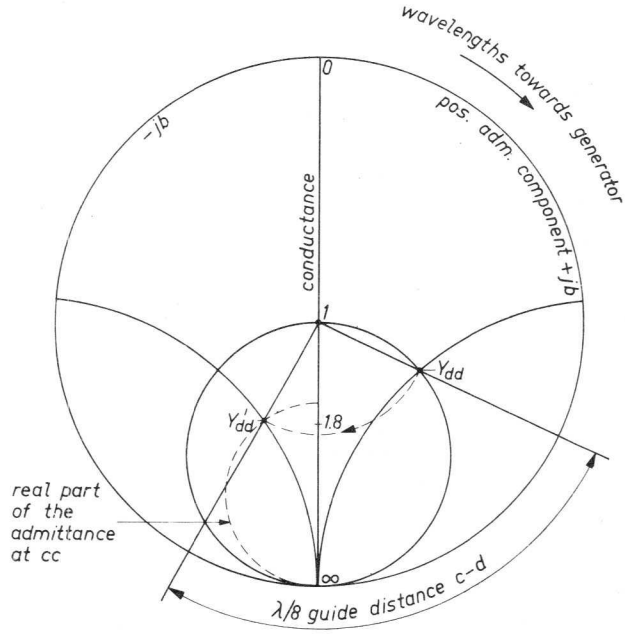

Fig.47. Smith chart illustrating the effect of varying the admittance G_2.

The admittance at the plane *dd* in Fig.46 is $Y = Y_0 + jB$. If the admittance B, which may be either positive or negative, is changed, the point P moves along the circle of the Smith chart. The real part of the admittance at the plane *cc* depends on B and may be greater or smaller than the surge admittance of the waveguide.

Owing to the incorporation of the variable admittance the resonant iris must be retuned to compensate the imaginary part of the admittance Y_{cc}.

It follows from eq.(3.2) that:

$$G_2^2 C_1 = 2C_2 Y_0^2 ,$$

where $G_2\sqrt{C_1}$ is constant. This gives for the 0.1 dB bandwidth:

$$B_{0.1\,\mathrm{dB}} = 0.276\,\frac{G_2}{C_2} = \text{constant} \cdot \frac{1}{\sqrt{C_1}} ,$$

which reveals that the bandwidth depends on the spread in the capacitance C_1.

5.4. ADJUSTMENT OF C_1

By incorporating a variable admittance Y between the resonant iris and the reflected anode circuit (see Fig.48), the reflected capacitance of C_1 can be modified. This may be explained as follows.

If the circuit Y_{cc} were omitted the 3 dB bandwidth of the circuit at the plane *aa* would be given by:

$$B = \frac{\text{real part of } Y_{aa}}{C_1} .$$

Since the real part of the admittance Y_{aa} can be influenced by the admittance Y_{bb}, the bandwidth can be adjusted in this way.

In the waveguide, at a distance $\lambda/2$ from the plane aa, a parallel resonant circuit will be observed. The damping of this circuit is to be attributed to the surge admittance Y_0, which remains unchanged.

It is thus seen that the bandwidth can be adjusted by means of the additional admittance Y, which amounts to the reflected capacitance C_1 being modified.

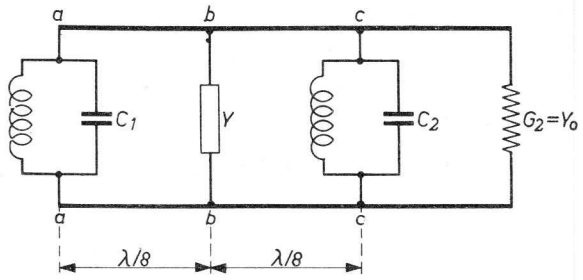

Fig.48. Waveguide provided with a variable admittance Y, between the resonant iris and the reflected anode circuit, for adjusting the capacitance C_1.

The 0.1 dB bandwidth of the circuit with the admittances $Y_{aa'}$ Y_{bb} and Y_{cc} will depend exclusively on B_2, viz:

$$B_{0.1\mathrm{dB}} = 0.276\ B_2 .$$

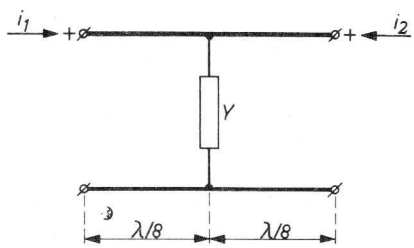

Fig.49. Representation of the coupling network with a variable admittance Y according to Fig.48.

To calculate the influence of Y, the coupling network may be represented by the circuit shown in Fig.49. The cascade matrix of this circuit is given by the product of the cascade matrices of the first $\lambda/8$ waveguide, of Y and of the second $\lambda/8$ waveguide, namely:

$$(a) = \begin{pmatrix} \frac{1}{\sqrt{2}} & \mathrm{j}\frac{1}{Y_0}\frac{1}{\sqrt{2}} \\ \mathrm{j}Y_0\frac{1}{\sqrt{2}} & \frac{1}{\sqrt{2}} \end{pmatrix} \cdot \begin{pmatrix} 1 & 0 \\ Y & 1 \end{pmatrix} \cdot \begin{pmatrix} \frac{1}{\sqrt{2}} & \mathrm{j}\frac{1}{Y_0}\frac{1}{\sqrt{2}} \\ \mathrm{j}Y_0\frac{1}{\sqrt{2}} & \frac{1}{\sqrt{2}} \end{pmatrix} =$$

$$= \begin{pmatrix} \frac{1}{2}\mathrm{j}\frac{Y}{Y_0} & \frac{\mathrm{j}}{Y_0} - \frac{1}{2}\frac{1}{Y_0}\cdot\frac{Y}{Y_0} \\ \frac{1}{2}Y + \mathrm{j}Y_0 & \frac{1}{2}\mathrm{j}\frac{Y}{Y_0} \end{pmatrix}.$$

By putting $Y = \mathrm{j}B$ and $Y/Y_0 = \mathrm{j}b$, the admittance matrix of the coupling network can be derived from the cascade matrix by means of the table of matrix interrelations given in Appendix IV of Article I, namely

$$Y = \begin{pmatrix} \frac{\frac{1}{2}bY_0 j}{1-\frac{1}{2}b} & \frac{Y_0 j}{1-\frac{1}{2}b} \\ \frac{Y_0 j}{1-\frac{1}{2}b} & \frac{\frac{1}{2}bY_0 j}{1-\frac{1}{2}b} \end{pmatrix} = \begin{pmatrix} Y_{11} & Y_{12} \\ Y_{21} & Y_{22} \end{pmatrix}$$

It will be assumed that Y_{11} is part of Y_1 and that Y_{22} is part of Y_2, and, moreover, that $Y_{11} + Y_1 = Y_I$ and $Y_{22} + Y_2 = Y_{II}$ are tuned to the reference frequency. The circuit then becomes as shown in Fig.50.

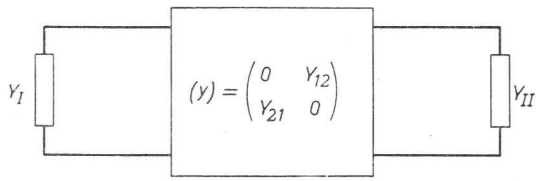

Fig.50. Representation of the coupling network in the case where Y_I and Y_{II} are tuned to the reference frequency.

The transfer admittance is now given by the expression:

$$-jY_0 Y_{tr} = \frac{Y_0^2}{\left(1-\frac{1}{2}b\right)^2} - G_2 \frac{C_1}{C_2} x'^2 + jG_2^2 \cdot \frac{C_1}{C_2} x' ,$$

so that the condition for a flat response curve becomes:

$$\frac{Y_0^2}{\left(1-\frac{1}{2}b\right)^2} = \frac{G_2^2 C_1}{2C_2} ,$$

or

$$Y_0^2 = \frac{G_2^2\left(1-\frac{1}{2}b\right)^2 C_1}{2C_2} .$$

If the lengths *ab* and *bc* of the waveguide are not exactly $\lambda/8$, the tuning of the resonant circuits must be readjusted. The 0.1 dB bandwidth will be given by eq.(4.1), namely 0.276 B_2.

5.5 SUMMARY

From the various methods for obtaining a flat response curve the adjustment of the capacitance C_1 discussed in Section 5.4 is chosen, for this method offers the following advantages:

(a) The 0.1 dB bandwidth of the filter for maximum flatness depends only on the bandwidth of the iris. Spread in the tube capacitances has no influence on the 0.1 dB bandwidth.

(b) For different inner conductors the 0.1 dB bandwidth depends exclusively on the bandwidth of the resonant iris.

(c) The geometrical dimensions of the amplifier can be kept small because of the short length of waveguide required.

6. PRACTICAL CONSIDERATIONS

Seen from the anode waveguide, a parallel tuned resonant circuit with a high quality factor is observed if the resonant iris and the admittance Y_{bb} are absent. If the cathode and anode circuit are tuned to the same frequency the location of this resonant circuit

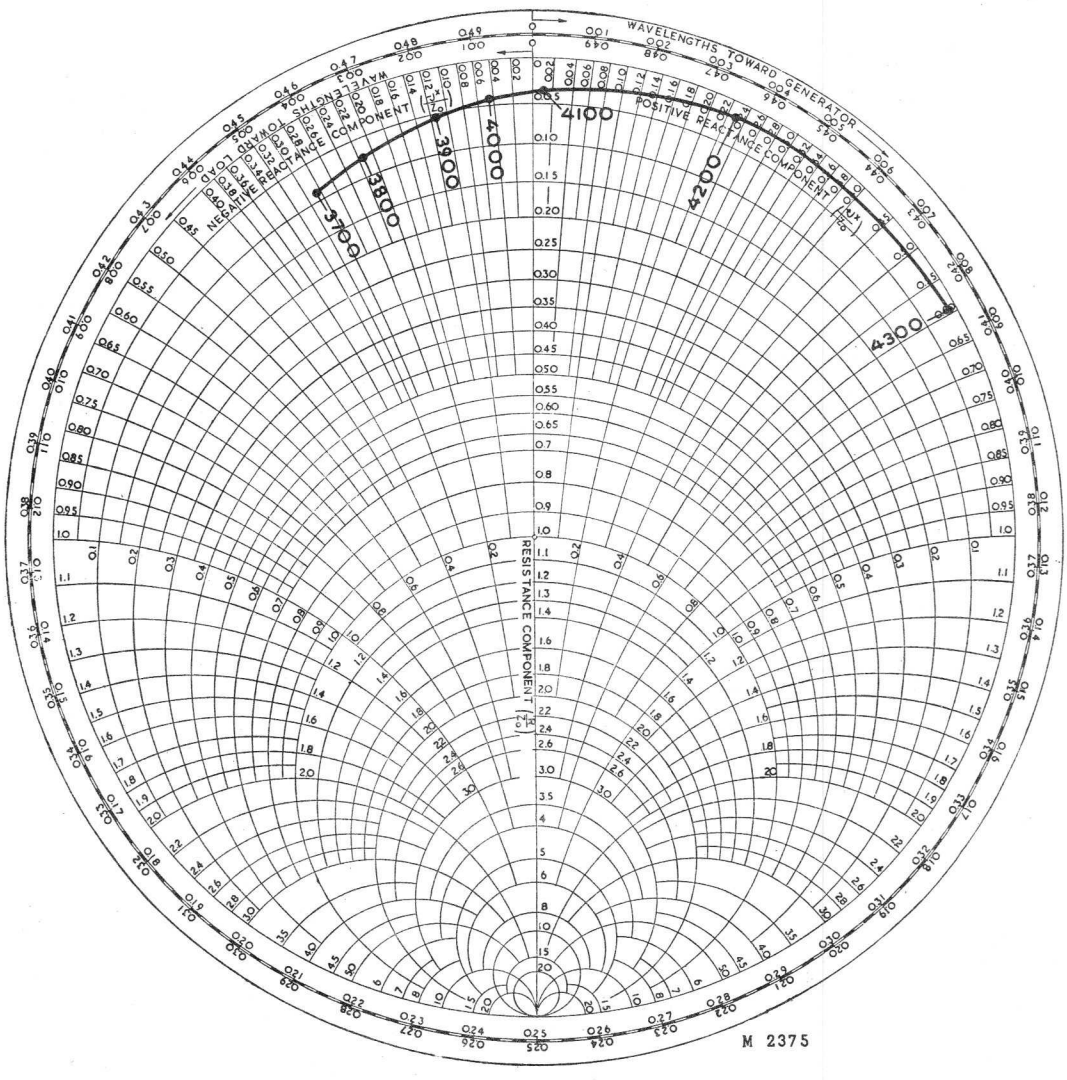

Fig.51. Smith chart showing the admittance at the location of the probe.

in the anode waveguide will depend on the frequency. The Smith chart shown in Fig.51 gives the admittance at the location of the probe. This chart reveals that the parallel tuned resonant circuit is located as indicated in Fig.52. At 4000 Mc/s this circuit is situated at a, whereas at 3700 Mc/s it is situated at a'', and at 4200 Mc/s at a'.

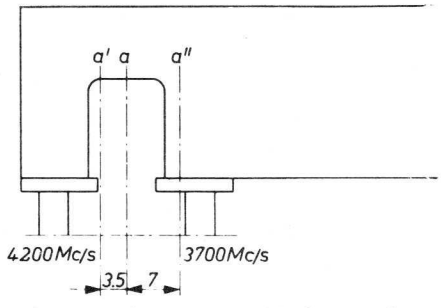

Fig.52. Location of the parallel tuned resonant circuit in the anode waveguide at different frequencies.

The shift of the resonant circuit is due to the fact that if the tuning of the anode cavity is changed, for example, from 4000 to 3700 Mc/s, the $\lambda/4$ transformer must be shifted upwards in the coaxial pair, the resonant circuit thus being shifted to the left.

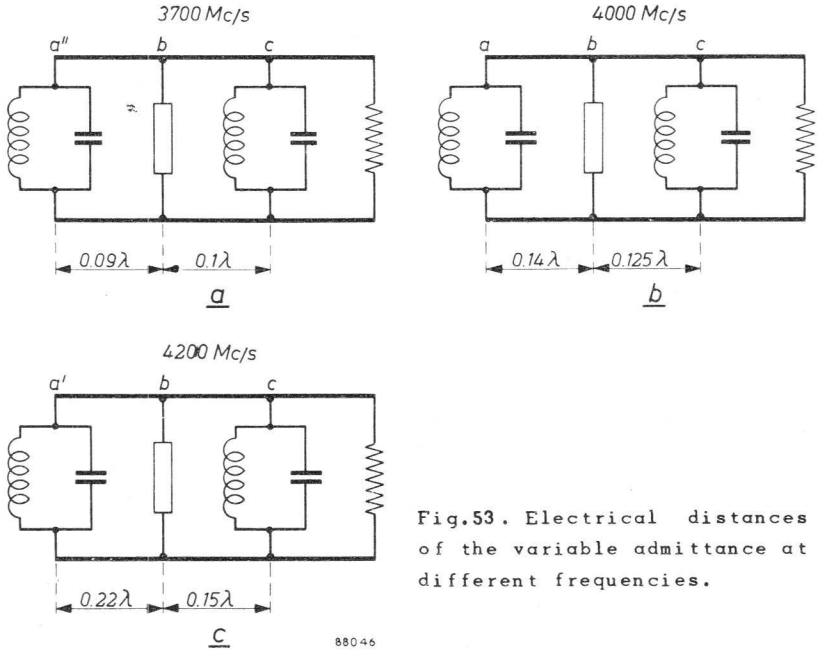

Fig.53. Electrical distances of the variable admittance at different frequencies.

The distance of the admittance Y from the reflected parallel circuit must be about $\lambda/8$ for all frequencies. The actual dimensions are a compromise allowing the response curve to be adjusted to maximum flatness within the band ranging from 3800 to 4200 Mc/s.

Figs 53*a*, *b* and c show the electrical distances of the variable admittance at several frequencies.

7. THE USE OF A UNIDIRECTIONAL COUPLER

If a unidirectional coupler is used, this can be combined with the amplifier to form a unit. The latter can be adjusted separately, and several units can then be connected in cascade, requiring no or very little readjustment. Fig.54 shows two possibilities, in which the unidirectional coupler forms part either of the anode circuit or of the cathode circuit.

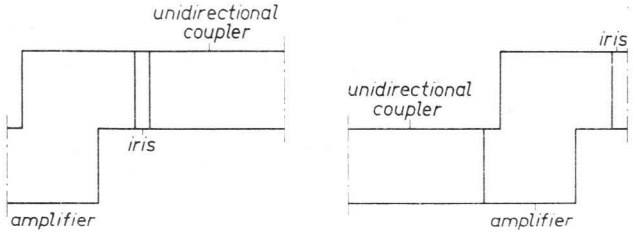

Fig.54. Representation of the two methods of combining the unidirectional coupler and amplifier.

If the V.S.W.R. of the unidirectional coupler were exactly 1, it would be immaterial which solution were chosen, but since the anode circuit is much more sensitive to detunings than the cathode circuit, it is preferable to assemble the unit so that the unidirectional coupler is connected to the anode side of the amplifier. It

has been shown that the adjustment of the unit can then be carried out very simply.

The use of the unidirectional coupler offers the following advantages:

(*a*) The amplifier stages can be adjusted individually and can be interchanged at random. In the case of a tube failure it will therefore not be necessary to readjust the entire installation.

(*b*) An arrangement is avoided in which the second resonant circuit of the filter, which is adjusted for maximum flatness, is formed by the cathode circuit of the following stage. This would be highly undesirable because this cathode circuit has a certain spread, which would result in a spread of the 0.1 dB flat bandwidth; by using a unidirectional coupler this 0.1 dB bandwidth is determined exclusively by the resonant iris. Moreover, small variations of the input capacitance of the following stage, such as may be caused by filament voltage fluctuations, will affect the tuning of the filter unless a unidirectional coupler is used.

(*c*) Looking into the amplifier from the aerial, the unidirectional coupler ensures a V.S.W.R. of exactly 1 at the centre frequency over a very wide band. If the V.S.W.R. were to differ appreciably from unity, as would be the case in the output stage if no unidirectional coupler were used, difficulties would probably be encountered with respect to the long-line effect of the aerial waveguide.

Measurements have revealed that the value of the bandwidth calculated in accordance with the above remarks are in good agreement with the actual bandwidth of the amplifier, deviations being less than 10%.

II. The Group Delay of the Amplifier

In Appendix I the matching of the anode circuit of the EC 56 amplifier to the following stage of a link system was discussed. The investigations were based on the assumption that the stages are correctly adjusted and not detuned.

In practice slight variations of the tube capacitances during the useful life of the tube are unavoidable, and it is the aim of this Appendix to analyse the effect of such variations on the group delay of the amplifier. If this group delay were to become excessive, the resulting phase distortion might give rise to serious interference (cross-talk in telephony or "ghosts" with TV reception).

In the amplifier dealt with, the anode circuit around the tubes forms part of a filter with maximum flatness, the 0.1 dB bandwidth being 55 or 27.5 Mc/s, and the band used having a width of 20 Mc/s. It is shown in this Appendix that, within the detuning interval, detuning of the second resonant circuit has a greater effect on the difference in the group delay than detuning of the anode circuit. Since, however, the second resonant circuit of the filter with maximum flatness is formed by a resonant iris, the second resonant circuit will be very stable.

If the anode circuit is detuned by 10 Mc/s the group delay in the 20 Mc/s band used will change 7.7×10^{-12} or 222×10^{-12} with a flat bandwidth of 55 or 27.5 Mc/s respectively. These calculated group delays have such low values that no difficulties need be expected during the life of the tubes.

1. SHORT DESCRIPTION OF THE ANODE CIRCUIT

For a detailed description of the anode circuit reference is made to Appendix I. The filter with maximum flatness consists of the reflected anode circuit represented by L_1 and C_1, a $\lambda/4$ waveguide, and - if a ferrite isolator is used - a resonant iris (L_2C_2). If no ferrite isolators are used for coupling the amplifiers, the second resonant circuit is formed by the cathode circuit of the following amplifier stage (see Fig.55).

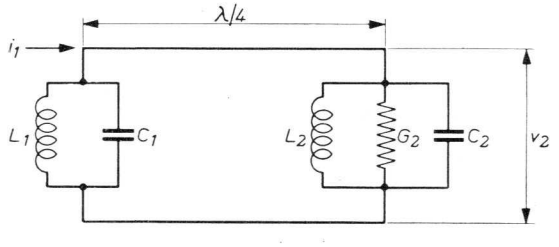

Fig.55. Representation of the anode circuit of an amplifying stage coupled directly by a $\lambda/4$ waveguide to the cathode circuit of the following stage. The bandwidth of this circuit is $B2 = G_2/C_2$.

According to eq. (1.4) of Appendix I the transfer admittance $Y_{tr} = i_1/V_2$ of the circuit is given by:

$$-jY_0Y_{tr} = Y_0^2 - 4p_1p_2C_1C_2 + 2G_2C_1(p_1 + p_2)x - G_2^2\frac{C_1}{G_2}x^2 - j2p_1G_2C_1 + jG_2^2\frac{C_1}{C_2}x, \tag{1.1}$$

where $x = (\omega/\omega_m - \omega_m/\omega)Q_2 = \beta Q_2$,

$p_1 = \omega_{01} - \omega_m$,

$p_2 = \omega_{02} - \omega_m$,

G_2 = conductance of the second resonant circuit, and

ω_m denotes the reference frequency and ω_{01} the resonant frequency of the circuit L_1C_1. The conductance of the first resonant circuit is assumed to be zero.

If both sides of eq.(1.1) are divided by $G_2{}^2C_1/C_2$ and he parameters

$$l_1 = \frac{2p_1}{B_2} \quad \text{and} \quad l_2 = \frac{2p_2}{B_2}$$

are introduced, eq.(1.1) becomes:

$$\frac{-jY_0Y_{tr}C_2}{G_2^2C_1} = \bar{N} = \frac{Y_0^2C_2}{G_2^2C_1} - l_1l_2 + (l_1 + l_2)x - x^2 - jl_1 + jx =$$

$$= \quad a \quad + \quad bx \quad + cx^2 + jd + jex. \tag{1.2}$$

If the two resonant circuits are transitionally coupled the conditions

$$\frac{Y_0^2C_2}{G_2^2C_1} = 0.5, \qquad l_1 = 0 \quad \text{and} \quad l_2 = 0.$$

must be satisfied (cf. eq.(3.2) of Appendix I. Therefore, in the case of a flat response curve:

$$\bar{N} = a + cx^2 + jex = 0.5 - x^2 + jx. \tag{1.3}$$

2. THE GROUP DELAY WITH TRANSITIONAL COUPLING

In Article I *) it is shown by eq. (10.13) that in the case where the coupling is transitional the group delay is given by:

$$\tau = \frac{2k}{\omega_m} \cdot \frac{ae - cex^2}{a^2 + c^2x^4},$$

whence

$$\tau = \frac{2Q_2}{\omega_m} \cdot \frac{0.5 + x^2}{0.25 + x^4} \simeq \frac{2Q_2}{\omega_m} \cdot 2(1 + 2x^2 - 4x^4), \tag{2.1}$$

the detuning x being given by:

$$\left(\frac{\omega}{\omega_m} - \frac{\omega_m}{\omega}\right)Q_2 = \frac{2\Delta\omega}{\omega_m} \cdot Q_2 = \frac{2\Delta\omega}{B_2}.$$

*) See footnote, p.41.

The group delay with transitional coupling will now be calculated for the case that the second resonant circuit has a bandwidth of 200 Mc/s or of 100 Mc/s, corresponding to a 0.1 dB bandwidth of 55 Mc/s or of 27.5 Mc/s respectively.

(a) B_2 = *200 Mc/s*

In this case the relation between the 3 dB bandwidth and the 0.1 dB bandwidth is given by (see eq. (4.1), Appendix I):

$$B_{01\,\mathrm{dB}} = 0.276\, B_{3\,\mathrm{dB}}\,.$$

It will be assumed that the band used has a width of ± 10 Mc/s, which, at B_2 = 200 Mc/s, gives:

$$x = \frac{2\Delta\omega}{B_2} = 0.1\,.$$

If the detuning is zero the group delay is:

$$\tau = \frac{4Q_2}{\omega_m} = \frac{4 \times 20}{2\pi \times 4 \times 10^9} = 3.2 \times 10^{-9}\ \mathrm{sec}\,.$$

This group delay is independent of the detuning and of no importance for the group delay distortion. For x = ± 0.1 the change in group delay is given by:

$$\Delta\tau = 3.2\,(0.02 - 0.0004)\,10^{-9} = 64 \times 10^{-12}\ \mathrm{sec}.$$

This maximum variation in the group delay is thus very small within the detuning interval x = ± 0.1 (see Fig.56).

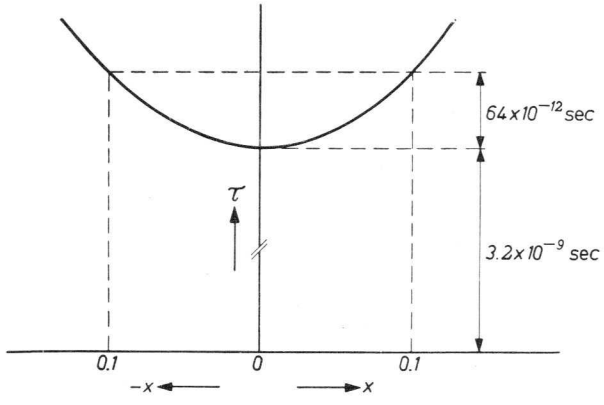

Fig.56. Response curve showing the variation of τ as a function of the detuning at B_2 = 200 Mc/s ($B_{0.1\ \mathrm{dB}}$ = 55 Mc/s). In the case of B_2 = 100 Mc/s ($B_{0.1\ \mathrm{dB}}$ = 27.5 Mc/s) the values become 6.4 x 10^{-9} and 474 x 10^{-12} instead of 3.2 x 10^{-9} and 64 x 10^{-12} respectively.

(b) B_2 = *100 Mc/s*

If the bandwidth of the second resonant circuit is 100 Mc/s ($B_{0\cdot1\ \mathrm{dB}}$ = 27.5 Mc/s) the quality factor of this circuit will be Q_2 = 4000/100 = 40. If the band used is again ± 10 Mc/s, the detuning

$$x = \frac{2\Delta\omega}{B_2} = \pm 0.2.$$

At zero detuning the group delay is 6.4 x 10^{-9} sec, which value is constant and independent of the frequency.

For $x = \pm 0.2$ the change in group delay is given by:

$$\Delta\tau = 6.4\,(0.08 - 0.0064)10^{-9} = 474 \times 10^{-12}\ \text{sec}.$$

2.1. DEPENDENCE OF THE CHANGE IN GROUP DELAY ON THE USED BANDWIDTH

The dependence of the change in group delay on the used bandwidth of the second resonant circuit may be determined as follows. The change in group delay as a function of the detuning may be expressed with reasonable accuracy (see eq. (2.1) with the fourth power and the constant term omitted):

$$\Delta\tau = \frac{4Q_2}{\omega_m} \cdot 2x^2,$$

where

$$\frac{Q_2}{\omega_m} = \frac{1}{B_2} \text{ and } x = \left(\frac{\omega}{\omega_m} - \frac{\omega_m}{\omega}\right) Q_2 = \frac{2\Delta\omega}{\omega_m} \cdot Q_2 = \frac{2\Delta\omega}{B_2}.$$

Hence

$$\Delta\tau = \frac{4 \times 2 \times 4\Delta\omega}{B_2{}^3} = \frac{32\Delta\omega}{B_2{}^3},$$

where $\Delta\omega$ is half the used band and B_2 is the bandwidth of the second resonant circuit, both quantities being expressed in c/s.

2.2. SUMMARY

With a single amplifier stage and a 0.1 dB flat bandwidth of 55 Mc/s and 27.5 Mc/s, the change in group delay is 64 x 10^{-12} sec and 474 x 10^{-12} sec respectively. If several amplifiers are used in cascade the group delays of the individual stages must be added.

The change in group delay, which can be compensated in the R.F. or I.F. part of the link system, depends strongly on the bandwidth, viz. it is proportional to the third power of the bandwidth. The change in group delay is proportional to the used band.

3. THE GROUP DELAY WITH A DETUNED ANODE CIRCUIT

It will be assumed that the second resonant circuit remains tuned to the reference frequency, and the anode circuit is detuned, so that $l_2 = 0$ and $l_1 \neq 0$.

If the anode circuit is detuned due to a change in the anode capacitance of the tube, the term $a = Y_0{}^2C_2/G_2{}^2C_1$ will also change. If the anode capacitance is increased by ΔC_1, then:

$$a = \frac{Y_0{}^2C_2}{G_2{}^2(C_1 + \Delta C_1)} = \frac{0.5}{1 + \dfrac{\Delta C_1}{C_1}}. \qquad (3.1)$$

It is possible to express $\Delta C_1/C_1$ in the following way in the parameters l_1 and Q_2:

$$\omega_{01}{}^2 = \frac{1}{L_1C_1},$$

hence, by differentiating:

$$2\omega_{01}\mathrm{d}\omega_{01} = -\frac{1}{L_1C_1}\cdot\frac{\mathrm{d}C_1}{C_1},$$

which gives:

$$\frac{\Delta C_1}{C_1} = -\frac{2\Delta\omega_{01}}{\omega_{01}} = -\frac{2p_1}{\omega_m} = -\frac{2p_1}{B_2}\cdot\frac{B_2}{\omega_m} = -\frac{l_1}{Q_2}.$$

$1/Q_2$ will have the same order of magnitude as l_1. The ratio l_1/Q_2 will be put equal to α^2, so that $a = 0.5/(1 - \alpha^2)$ and the term a becomes:

$$a = 0.5\,(1 + \alpha^2 + \alpha^4). \qquad (3.2)$$

At $l_2 = 0$ the transfer admittance can be expressed by:

$$N = 0.5\,(1 + \alpha^2 + \alpha^4) + l_1x - x^2 - \mathrm{j}l_1 + \mathrm{j}x =$$

$$= a + bx + cx^2 + \mathrm{j}d + \mathrm{j}ex.$$

According to eq. (10.5) of Article I the group delay is given by:

$$\tau = \frac{2k}{\omega_m}\cdot\frac{ae - bd - 2cdx - cex^2}{(a + bx + cx^2)^2 + (d + ex)^2},$$

whereas the group delay for the detuned anode circuit is:

$$\tau_{\mathrm{det}} = \frac{2Q_2}{\omega}\cdot\frac{0.5\,(1 + \alpha^2 + \alpha^4) + (x - l_1)^2}{\{0.5\,(1 + \alpha^2 + \alpha^4) + l_1x - x^2\}^2 + (x - l_1)^2}. \qquad (3.3)$$

As shown elsewhere *) this expression may be rewritten:

$$\tau_{\mathrm{det}} = \frac{2Q_2}{\omega_m}\cdot 2\Big[1 - \alpha^2 - 2l_1^2 + 8\alpha^2l_1^2 - \alpha^4 + 8l_1^2 + 2x^2 - 4x^4 +$$

$$+ 4\{4l_1x^3 - 3l_1^2x^2 - 2(\alpha^2l_1 + l_1^3)x\}\Big]. \qquad (3.4)$$

Attention is drawn to the fact that, if the detuning is due to a change in the inductance of the circuit, $\alpha = 0$.

3.1. THE CHANGE OF THE GROUP DELAY IF THE CIRCUIT IS COMPENSATED FOR TRANSITIONAL COUPLING

In a link system the group delay of the R.F. part is often compensated in the I.F. part of the system. A network is then used that introduces the following group delay as a function of the detuning x:

$$\tau = -\frac{2Q_2}{\omega_m}\cdot 2(1 + 2x^2 - 4x^4),$$

i.e. equal to but differing in sign from the group delay that occurs in the R.F. part if the anode circuit is correctly tuned and the response curve is flat.

*) Electr. Appl. Vol.16, p.144 1955/1956 (No.4).

The change in group delay is *)

$$\tau_d + \tau_c = \frac{2Q_2}{\omega_m} \cdot 2 \left[(-a^2 - 2l_1^2 + 8a^2 l_1^2 - a^4 + 8l_1^4) + \right.$$
$$\left. + 4 \left\{ 4l_1 x^3 - 3l_1^2 x^2 - 2(a^2 l_1 + l_1^3)\, x \right\} \right]$$

The term $(-a^2 - 2l_1^2 + 8a^2 l_1^2 - a^4 + 8l_1^4)$ is independent of the frequency and will only give rise to a constant delay without introducing any group delay distortion. The change of the group delay as a function of the detuning is therefore given by:

$$\Delta\tau = \frac{2Q_2}{\omega_m} \cdot 8 \left\{ 4 l_1 x^3 - 3 l_1^2 x^2 - 2(a^2 l_1 + l_1^3) x \right\} =$$
$$= \frac{16 Q_2}{\omega_m} \cdot l_1^4 \left\{ 4 \left(\frac{x}{l_1}\right)^3 - 3 \left(\frac{x}{l_1}\right)^2 - 2 \left(\frac{a^2}{l_1^2} + 1\right) \cdot \frac{x}{l_1} \right\}. \qquad (3.5)$$

Putting $x/l_1 = u$ gives:

$$\Delta\tau = \frac{16 Q_2}{\omega_m} \cdot l_1^4 \left\{ 4u^3 - 3u^2 - 2 \left(\frac{a^2}{l_1^2} + 1\right) u \right\}. \qquad (3.5a)$$

Using this formula, the difference between the maximum and the minimum values of $\Delta\tau$ in the detuning interval concerned will now be investigated. For this purpose it will be useful to put:

$$4u^3 - 3u^2 - 2 \left(\frac{a^2}{l_1^2} + 1\right) u = W, \qquad (3.6)$$

in which:

$$\frac{a^2}{l_1^2} = \frac{l_1}{Q_2} \cdot \frac{1}{l_1^2} = \frac{1}{l_1 Q_2},$$

l_1 being equal to $2p_1/B_2$.

Denoting the difference between the maximum and the minimum values of the group delay in the frequency interval considered by $\Delta\tau_{max}$ and the difference between the maximum and minimum values of W in this interval by ΔW_{max}, then the value of $\Delta\tau_{max}$ can be calculated from the expression:

$$\tau_{max} = \frac{16 Q_2}{\omega_m} \cdot l_1^4 \Delta W_{max}. \qquad (3.7)$$

The value of $\Delta\tau_{max}$ will first be calculated for the case where the detuning of the anode circuit is 10 Mc/s and the used band has a width of 20 Mc/s.

If it is assumed that the anode capacitance increases so that $p_1 = \omega_{0.1} - \omega_m$ becomes negative, the coefficient l_1 becomes -2 x 10/200 = -0.1, whilst $Q_2 = \omega_m/B_2$ becomes 4000/200 = 20. Hence:

$$a^2 = \frac{1}{l_1 Q_2} = -\frac{1}{0.1 \times 20} = -0.5.$$

*) Electr. Appl. Vol 16, p.144, 1955/1956 (No.4).

Substitution of these values for l_1 and α^2 in eq. (3.6) gives:

$$W = 4u^3 - 3u^2 - u, \qquad (3.8)$$

where $u = x/l_1$, $x = 2\Delta\omega/B_2$ and $l_1 = 2p_1/B_2$, whence $u = \Delta\omega/p_1$. This function has been plotted in Fig.57.

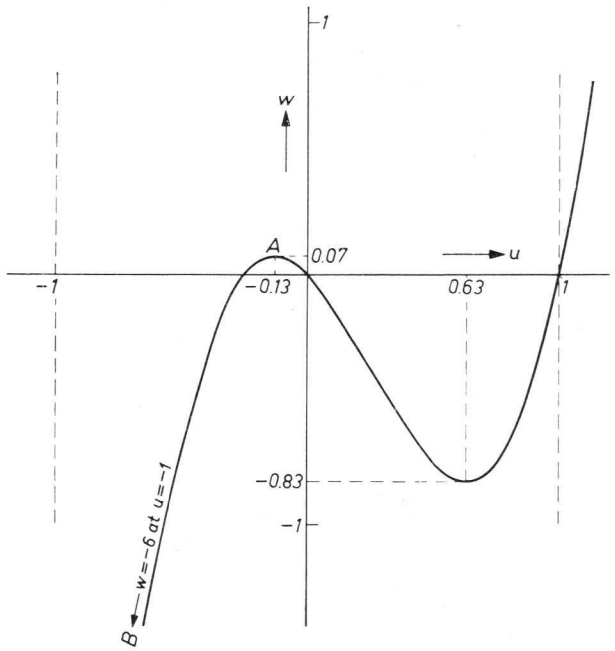

Fig.57. Graphical representation of eq. (3.8).

Since the used band has a total width of 20 Mc/s, $\Delta\omega$ is $\pm 2\pi$ times 10 Mc/s, the detuning p_1 of the anode circuit then being 2π x 10 Mc/s. The interval thus ranges from $u = +1$ to $u = -1$. Within this interval, W is a maximum at point A ($W = 0.07$) and a minimum at point B ($W = -6$). The value of ΔW_{max} is therefore 6.07. Hence:

$$\Delta\tau_{max} = \frac{16Q_2}{\omega_m} \cdot l_1^4 \cdot 6.07 = \frac{16 \times 20}{2\pi \times 4 \times 10^9} \cdot 0.1^4 \times 6.07 = 7.7 \times 10^{-12} \text{ sec.}$$

The calculation of $\Delta\tau_{max}$ for the case where the detuning of the anode circuit is 5 Mc/s instead of 10 Mc/s is carried out on the same lines. The value of $l_1 = 2p_1/B_2$ is now -2 x 5/200 = -0.05, and the interval is given by

$$u = \frac{x}{l_1} = \frac{2\Delta\omega}{p_1} = \pm 2,$$

whilst

$$\frac{\alpha^2}{l_1^2} = \frac{1}{l_1 Q_2} = -\frac{1}{0.05 \times 20} = -1.$$

Eq (3.2) is thus simplified in this case to:

$$W = 4u^3 - 3u^2. \qquad (3.9)$$

This function has been plotted in Fig.58. It follows from this graph that only the values for $u = \pm 2$ are important, which gives for $\Delta W_{max} = 64$. Hence:

$$\Delta\tau_{max} = \frac{16Q_2}{\omega_m} \cdot l_1^4 \cdot 64 = 12.7 \times 0.05^4 \times 64 \times 10^{-9} = 5.1 \times 10^{-12} \text{ sec.}$$

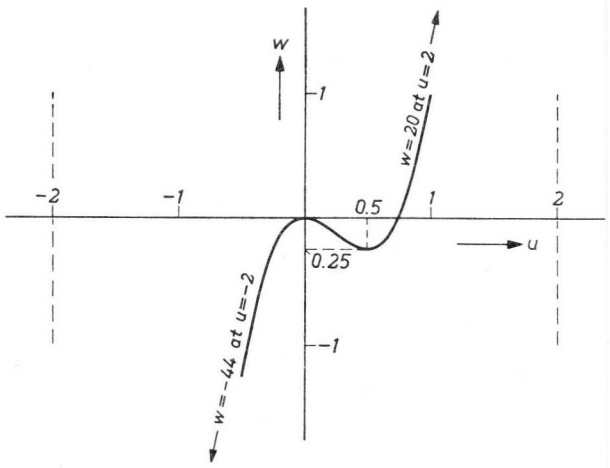

Fig.58. Graphical representation of eq. (3.9).

Finally, it will be assumed that the detuning of the anode circuit is 1 Mc/s, the used band being again 20 Mc/s. In this case p_1 = -1 Mc/s and B_2 = 200 Mc/s, which gives

$$l_1 = \frac{2p_1}{B_2} = -\frac{2 \times 1}{200} = -0.01$$

and

$$\frac{1}{l_1 Q_2} = \frac{\alpha^2}{l_1^2} = -\frac{1}{0.01 \times 20} = -5,$$

so that eq. (3.2) becomes:

$$W = 4u^3 - 3u^2 + 8u,$$

the interval being:

$$u = \pm \frac{\Delta\omega}{p_1} = \pm \frac{10}{1} = \pm 10.$$

Only the values of W for u = ± 10 will be of importance in this case. At u = +10, W = 3780 and at u = -10, W = -4380, which gives ΔW_{max} = 8160.
Consequently,

$$\Delta\tau_{max} = \frac{16Q_2}{\omega_m} \cdot l_1^4 \cdot 8160 = 1.05 \times 10^{-12} \text{ sec.}$$

The value of $\Delta\tau_{max}$ will now be calculated for the case where the detuning of the anode circuit is 10 Mc/s and the used band has a width of 20 Mc/s, it being assumed that Q_2 = 40.

As indicated above, it may be written:

$$l_1 = \frac{2p_1}{B_2} = -\frac{2 \times 10}{100} = -0.2$$

(the capacitance increases), and

$$x = \frac{2\Delta\omega}{B_2} = \pm \frac{2 \times 10}{100} = \pm 0.2.$$

Hence:

$$\frac{\alpha^2}{l_1^2} = \frac{1}{l_1 Q_2} = -\frac{1}{0.2 \times 40} = -0.125\,,$$

so that the expression for W (see eq (3.6)) becomes:

$$W = 4u^3 - 3u^2 - 1.75u\,, \qquad (3.10)$$

whilst the interval is given by $u = \Delta\omega/p_1 = \pm 1$. The value of W as a function of u has been plotted in Fig.59.

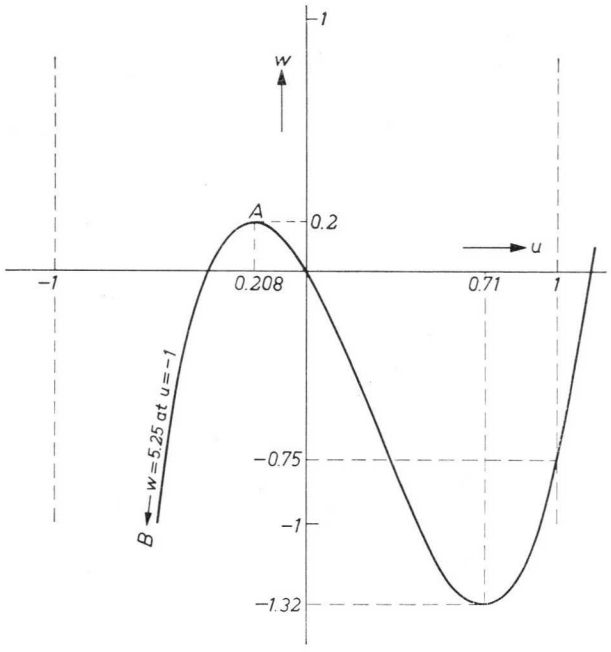

Fig.59. Graphical representation of eq. (3.10).

ΔW_{max} is given by the difference of the values of W at the points A and B, namely 5.25 + 0.2 = 5.45. In this case, therefore:

$$\Delta\tau_{max} = \frac{16Q_2}{\omega_m} \cdot l_1^4 \cdot \Delta W_{max} = \frac{16 \times 40}{2\pi \times 4 \times 10^9} \cdot 0.2^4 \times 5.45 = 222 \times 10^{-12}\ \text{sec.}$$

If the detuning of the anode circuit is 5 Mc/s instead of 10 Mc/s,

$$l_1 = \frac{2p_1}{B_2} = -\frac{2 \times 5}{100} = -0.1$$

and

$$\frac{\alpha^2}{l_1^2} = \frac{1}{l_1 Q_2} = -\frac{1}{0.1 \times 40} = -0.25\,.$$

Since $x = \pm 0.2$, this gives:

$$W = 4u^3 - 3u^2 - 1.5u.$$

The interval $u = \Delta\omega/p_1 = \pm 2$, so that the extreme values of W are -1.15 (at u = +0.68) and +0.24 (at u = -0.18). For u = +2 and u = -1 the values of W are +17 and -41 respectively, which gives ΔW_{max} = 17 + 41 = 58 in this interval, whence:

$$\Delta\tau_{max} = \frac{16 \times 40}{2\pi \times 4 \times 10^9} \cdot 0.1^4 \times 58 = 74 \times 10^{-12}\ \text{sec.}$$

If the detuning of the anode circuit is only 1 Mc/s,

$$l_1 = \frac{2p_1}{B_2} = -\frac{2 \times 1}{100} = -0.02$$

and

$$\frac{\alpha^2}{l_1^2} = \frac{1}{l_1 Q^2} = -\frac{1}{0.02 \times 40} = -1.25 .$$

In this case, too, x = ± 0.2, so that

$$W = 4u^3 - 3u^2 + 0.5u .$$

The interval $u = \Delta\omega/p_1 = \pm 10$, so that for the extreme values of this interval W becomes +3705 and -4305, ΔW_{max} thus being 8010. Hence:

$$\tau_{max} = \frac{16 \times 40}{2\pi \cdot 4 \times 10^9} \cdot 0.024 \times 8010 = 32.6 \times 10^{-12} \text{ sec.}$$

3.2. INFLUENCE OF B_2 ON THE MAXIMUM DIFFERENCE IN THE GROUP DELAY

It will now be investigated what influence the bandwidth of the second resonant circuit has on the maximum difference in the group delay if the anode circuit is detuned. According to eq. (3.5a)

$$\Delta\tau = \frac{16Q_2}{\omega_m} \cdot l_1^4 \left\{ 4u^3 - 3u^2 - 2\left(\frac{\alpha^2}{l_1^2} + 1\right) u \right\},$$

where

$$\frac{\alpha^2}{l_1^2} = \frac{1}{l_1 Q_2} = \frac{B_2}{2p_1 Q_2} .$$

If the influence of the latter term is neglected,

$$W = 4u^3 - 2u^2 - 2\left(\frac{\alpha^2}{l_1^2} + 1\right) u$$

will be a function of u only. Since $u = \Delta\omega/p_1$, in which $\Delta\omega$ is half the used band and p_1 is the detuning of the anode circuit expressed in 2π times the frequency (in Mc/s), the parameter W and also ΔW_{max} will hardly be influenced by a change of the bandwidth of the second resonant circuit. Hence

$$\Delta\tau_{max} = \frac{16Q_2}{\omega_m} \cdot \left(\frac{2p_1}{B_2}\right)^4 \cdot \Delta W_{max} ,$$

where $Q_2/\omega_m = 1/2\pi B_2$, may be written:

$$\Delta\tau_{max} = \text{constant} \cdot \frac{p_1^4}{B_2^5} \cdot \Delta W_{max} .$$

A rough estimate thus reveals that $\Delta\tau_{max}$ will be inversely proportional to the fifth power of B_2. Since it is fairly difficult to obtain large bandwidths at intermediate frequencies it may be expected that at these frequencies trouble is much more likely to be experienced due to group delay distortion than at 4000 Mc/s.

4. THE GROUP DELAY WITH DETUNING OF THE SECOND RESONANT CIRCUIT

When the second resonant circuit is detuned $l_1 = 0$ but $l_2 \neq 0$. If the capacitance of the resonant circuit of the filter with maximum flatness changes, the transfer admittance (see eq (1.2)). may therefore be expressed by:

$$N = \frac{Y_0^2(C_2 + \Delta C_2)}{G_2^2 C_1} + l_2 x - x^2 + jx = 0.5\left(1 + \frac{\Delta C_2}{C_2}\right) + l_2 x - x^2 + jx .$$

Substitution of:

$$\frac{\Delta C_2}{C_2} = -\frac{l_2}{Q_2} = \alpha^2$$

gives:

$$\begin{aligned} N &= 0.5\,(1 + \alpha^2) + l_2 x - x^2 + jx \\ &= a + bx + cx + jex. \end{aligned}$$

According to eq.(10.5) of Article I the group delay is:

$$\tau = \frac{2k}{\omega_m} \cdot \frac{ac - bd - 2cdx - cex^2}{(a + bx + cx^2)^2 + (d + ex)^2},$$

which gives:

$$\tau = \frac{2Q_2}{\omega_m} \cdot \frac{0.5\,(1 + \alpha^2) + x^2}{\{0.5(1 + \alpha^2) + l_2 x - x^2\}^2 + x^2}. \qquad (4.1)$$

It can be derived from this expression *) that:

$$\tau_{\text{det}} = \frac{2Q_2}{\omega_m} \cdot 2\,(1 + 2x^2 - 4x^4 - \alpha^2 + \alpha^4 - 4l_2 x + 8\alpha^2 l_2 x + 12 l_2^2 x^2).$$

If l_2 and x are smaller than unity so that $8\alpha^2 l_2 x + 12 l_2^2 x^2$ can be neglected compared with $-4l_2 x$, this expression may be simplified to:

$$\tau_{\text{det}} = \frac{2Q_2}{\omega_m} \cdot 2\,(1 + 2x^2 - 4x^4 - \alpha^2 - 4l_2 x). \qquad (4.2)$$

4.1. EFFECT OF COMPENSATING THE CIRCUIT FOR THE TRANSITIONAL CASE

If the second resonant circuit and the anode circuit are correctly tuned, the group delay is (see eq.(4.2)):

$$\tau = \frac{2Q_2}{\omega_m} \cdot 2\,(1 + 2x^2 - 4x^4).$$

It will be assumed that this group delay of the R.F. part is compensated in the I.F. part. The change of the group delay as a function of the detuning x is then given by (see eq.(4.2)):

$$\Delta\tau = \frac{2Q_2}{\omega_m} \cdot 2\,(-4l_2 x),$$

from which it follows that:

$$|\Delta\tau| = \frac{16Q_2}{\omega_m} \cdot l_2 x. \qquad (4.3)$$

*) see Electr.Appl. Vol 16, p. 145, 1955/1956 (No.4).

By means of this expression the value of $\Delta\tau_{max}$ can be calculated. It will first be assumed that the 0.1 dB bandwidth is 55 Mc/s so that B_2 = 200 Mc/s, the quality factor Q_2 of the second resonant circuit being 4000/200 = 20.

According to eq.(4.3), $\Delta\tau$ is proportional to the detuning of the second resonant circuit and the used band. If this band is again taken to be 20 Mc/s, this gives:

$$x = \pm \frac{20}{200} = \pm 0.1 ,$$

whilst the factor

$$\frac{16Q_2}{\omega_m} = \frac{16 \times 20}{2\pi \times 4} . 10^{-9} = 12.75 \times 10^{-9} \text{ sec.}$$

The resulting values of $\Delta\tau_{max}$ are tabulated below for three values of detuning of the second resonant circuit:

detuning	l_2	$\Delta\tau_{max}$	
10 Mc/s	0.1	255×10^{-12}	sec
5 Mc/s	0.05	127×10^{-12}	sec
1 Mc/s	0.01	25×10^{-12}	sec

If the 0.1 dB bandwidth is only 27.5 Mc/s and B_2 = 100 Mc/s, Q_2 being 4000/100 = 40:

$$x = \pm \frac{20}{100} = \pm 0.2 ,$$

whilst the factor $16Q_2/\omega_m$ becomes 25.5 x 10^{-9} sec. This gives:

detuning	l_2	$\Delta\tau_{max}$	
10 Mc/s	0.2	1×10^{-9}	sec
5 Mc/s	0.1	0.5×10^{-9}	sec
1 Mc/s	0.02	0.1×10^{-9}	sec

4.2. INFLUENCE OF B_2 ON THE MAXIMUM DIFFERENCE IN GROUP DELAY

According to eq.(4.3):

$$\Delta\tau_{max} = \text{constant} \cdot \frac{Q_2}{\omega_m} \cdot l_2 x ,$$

which, in the case of

$$l_2 = \frac{2p_2}{B_2} , \qquad x = \frac{2\Delta\omega}{B} \quad \text{and} \quad Q_2 = \frac{\omega_{02}}{B_2}$$

may be written:

$$\Delta\tau_{max} = \text{constant} \cdot \frac{1}{B_2} \cdot \frac{\omega_{02}}{B_2} \cdot \frac{\Delta\omega}{B_2} = \text{constant} \cdot \frac{\omega_{02}\Delta\omega}{B_2^3} .$$

This expression reveals that $\Delta\tau_{max}$ is inversely proportional to the third power of B_2.

5. EFFECT OF INCORRECT COUPLING ON THE GROUP DELAY

5.1. THE RESPONSE CURVE AND THE FORMULA FOR THE GROUP DELAY

If the response curve is symmetrical, then, according to eq.(1.2), the transfer admittance of the total circuit is given by:

$$\bar{N} = \frac{Y_0^2 C_2}{G_2 C_1} - x^2 + jx ,$$

the term $Y_0^2 C_2 / G_2 C_1$ being 0.5 if the circuits are transitionally coupled (see eq.(3.2) of Appendix I).

If the coupling is incorrect the factor 0.5 will assume a different value, say $0.5(1 + k)$, the change of the coupling amounting to k%. In that case the general expression

$$\bar{N} = a + cx^2 + jex$$

becomes:

$$\bar{N} = 0.5\,(1 + k) - x^2 + jx,$$

the modulus of N being:

$$|\bar{N}|^2 = \{0.5(1 + k) - x^2\}^2 + x^2 = 0.25(1 + k)^2 - kx^2 + x^4 .$$

The extreme values of this modulus can be found by putting $d|N|^2/dx = 0$, which gives:

$$-2kx + 4x^3 = 0 .$$

The value of x may thus assume two different values, namely $x = 0$, or $x = \sqrt{k/2}$, in which case either:

$$|\bar{N}| = 0.5\,(1 + k) \quad \text{and} \quad \frac{1}{|\bar{N}|} = \frac{2}{1 + k},$$

or

$$|\bar{N}| = 0.5\,\sqrt{1 + 2k} \quad \text{and} \quad \frac{1}{|\bar{N}|} = \frac{2}{\sqrt{1 + 2k}}$$

respectively. This response curve is represented by the fully drawn line in Fig.60. The difference d between the top and the dip of the response curve is therefore given by:

$$d = \frac{2}{\sqrt{1 + 2k}} + \frac{2}{1 + k} = 2\,(1 - k + \frac{3}{2}k^2 \ldots - 1 + k - k^2 \ldots) \simeq k^2 .$$

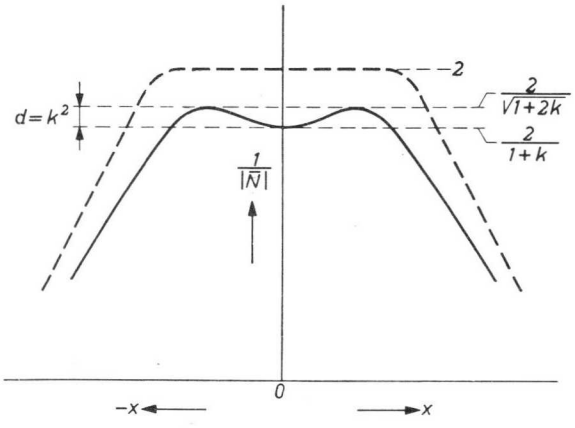

Fig.60. Response curve with incorrect coupling (fully drawn line). The difference between the top and the dip of this curve is denoted by d.

Since the difference is referred to the response curve $1\sqrt{|N|} = 2$, the difference d referred to the response curve $1\sqrt{|N|} = 1$ will be $k^2/2$ if the coupling changes by k%.

The group delay can be calculated from eq.(10.8) on p. 94 of Article I:

$$\tau = \frac{2k}{\omega_m} \cdot \frac{ae - cex^2}{a^2 + (2ac + e^2)\,x^2 + c^2x^4},$$

which gives

$$\tau = \frac{2Q_2}{\omega_m} \cdot \frac{0.5(1+k) + x^2}{0.25(1+k)^2 - kx^2 + x^4} = \frac{4Q_2}{\omega_m} \cdot \frac{1 + k + 2x^2}{1 + 2k + k^2 - 4kx^2 + 4x^4}. \qquad (5.1)$$

5.2. THE INFLUENCE OF AN INCORRECT COUPLING OF 20%

To give an idea of the change in the group delay as a result of the coupling being incorrect, it will be assumed that the latter is too tight and amounts to 20%. Instead of being flat, the response curve will then show a dip, and the difference between the top and the valley of the response curve will be:

$$\frac{\frac{k^2}{2}}{1+k} \cdot 100 = \frac{\frac{0.2^2}{2}}{1+0.2} \cdot 100 = 2.4\%.$$

The change in the group delay in the detuning interval will be:

$$\Delta\tau = \frac{4Q_2}{\omega_m}\left(-\frac{1+k}{1+2k+k^2} + \frac{1+k+2x^2}{1+2k+k^2-4kx^2+4x^4}\right). \qquad (5.2)$$

If the 0.1 dB bandwidth is 55 Mc/s (B_2 = 200 Mc/s) and the total width of the used band is 20 Mc/s, the detuning interval is given by $x = 2\Delta\omega/B_2 = \pm 0.1$. If the quality factor of the second resonant circuit is again assumed to be 20, the change in the group delay thus becomes according to eq.(5.2):

$$\Delta\tau = \frac{80}{2\pi \times 4 \times 10^9}\left(-\frac{1.20}{1.44} + \frac{1.22}{1.43}\right) = 57 \times 10^{-12}\ \text{sec}.$$

At a 0.1 dB bandwidth of 27.5 Mc/s (B_2 = 100 Mc/s) and a total width of the used band of 20 Mc/s, the detuning interval is $x = 2\Delta\omega/B_2 = \pm 0.2$. Assuming the quality factor of the second resonant circuit to be 40 in this case, the change in the group delay now is:

$$\Delta\tau = \frac{4 \times 40}{2\pi \times 4 \times 10^9}\left(-\frac{1.20}{1.44} + \frac{1.28}{1.41}\right) = 520 \times 10^{-12}\ \text{sec}.$$

6. SUMMARY OF THE RESULTS

In the table below the calculated values of the maximum difference in the group delay $\Delta\tau_{max}$ are recapitulated for various conditions, it being assumed that the used band has a total width of 20 Mc/s.

The table reveals that the changes in the group delay for various degrees of detuning of the circuits of the filter with maximum flatness and at an incorrect adjustment of the coupling are so small that they may as a rule be neglected compared with the group delay encountered in the I.F. amplifier of the link system.

conditions	$\Delta\tau_{max}$ in seconds	
	$B_{0.1dB}$ = 55 Mc/s B_2 = 200 Mc/s Q_2 = 20	$B_{0.1dB}$ = 27.5 Mc/s B_2 = 100 Mc/s Q_2 = 40
I.F. circuit not compensated for the group delay	64×10^{-12}	474×10^{-12}
Anode circuit detuned and circuit compensated for the group delay in the transitional case:		
detuning 10 Mc/s	7.7×10^{-12}	222×10^{-12}
detuning 5 Mc/s	5.1×10^{-12}	74×10^{-12}
detuning 1 Mc/s	1×10^{-12}	33×10^{-12}
Second resonant circuit detuned and circuit compensated for the group delay in the transitional case:		
detuning 10 Mc/s	255×10^{-12}	1×10^{-9}
detuning 5 Mc/s	127×10^{-12}	0.5×10^{-9}
detuning 1 Mc/s	25×10^{-12}	0.1×10^{-9}
Incorrect coupling, the difference between the (over-transitional) incorrect coupling and the transitional coupling being 20%; 2.4% difference between the top and the dip of the response curve	57×10^{-12}	520×10^{-12}

M 2409

Printed in Holland

20/303/D/E-11-'56